ARTICLE

NFIB Haploinsufficiency Is Associated with Intellectual Disability and Macrocephaly

Ina Schanze,[1,33] Jens Bunt,[2,33,*] Jonathan W.C. Lim,[2] Denny Schanze,[1] Ryan J. Dean,[2] Marielle Alders,[3] Patricia Blanchet,[4] Tania Attié-Bitach,[5] Siren Berland,[6] Steven Boogert,[1] Sangamitra Boppudi,[1] Caitlin J. Bridges,[1] Megan T. Cho,[7] William B. Dobyns,[8] Dian Donnai,[9] Jessica Douglas,[10] Dawn L. Earl,[11] Timothy J. Edwards,[2,12] Laurence Faivre,[13,14] Brieana Fregeau,[15] David Genevieve,[4] Marion Gérard,[16] Vincent Gatinois,[4] Muriel Holder-Espinasse,[17,18]

(Author list continued on next page)

The nuclear factor I (NFI) family of transcription factors play an important role in normal development of multiple organs. Three NFI family members are highly expressed in the brain, and deletions or sequence variants in two of these, *NFIA* and *NFIX*, have been associated with intellectual disability (ID) and brain malformations. *NFIB*, however, has not previously been implicated in human disease. Here, we present a cohort of 18 individuals with mild ID and behavioral issues who are haploinsufficient for *NFIB*. Ten individuals harbored overlapping microdeletions of the chromosomal 9p23-p22.2 region, ranging in size from 225 kb to 4.3 Mb. Five additional subjects had point sequence variations creating a premature termination codon, and three subjects harbored single-nucleotide variations resulting in an inactive protein as determined using an *in vitro* reporter assay. All individuals presented with additional variable neurodevelopmental phenotypes, including muscular hypotonia, motor and speech delay, attention deficit disorder, autism spectrum disorder, and behavioral abnormalities. While structural brain anomalies, including dysgenesis of corpus callosum, were variable, individuals most frequently presented with macrocephaly. To determine whether macrocephaly could be a functional consequence of *NFIB* disruption, we analyzed a cortex-specific *Nfib* conditional knockout mouse model, which is postnatally viable. Utilizing magnetic resonance imaging and histology, we demonstrate that *Nfib* conditional knockout mice have enlargement of the cerebral cortex but preservation of overall brain structure and interhemispheric connectivity. Based on our findings, we propose that haploinsufficiency of *NFIB* causes ID with macrocephaly.

Introduction

The nuclear factor one (NFI) site-specific DNA-binding proteins represent a family of transcription factors important for the development of multiple organ systems including the brain.[1–9] Recent reports have highlighted a role for two *NFI* family members, *NFIA* (MIM: 600727) and *NFIX* (MIM: 164005), in individuals with intellectual disability (ID). Deletions of chromosome 1p32p31 (chromosome 1p32p31 deletion syndrome [MIM: 613735]) as well as deletions or sequence variants of *NFIA* lead to a phenotype with developmental delay, macrocephaly, ID, dysgenesis of the corpus callosum, ventriculomegaly or congenital hydrocephalus, and craniofacial dysmorphisms.[10–19] Haploinsufficiency of *NFIX* causes Sotos syndrome 2 or Malan syndrome (MIM: 614753), which is characterized by developmental delay, macrocephaly, ID, postnatal overgrowth, and mild craniofacial anomalies.[20–26] In addition, specific sequence variants affecting the 3′ region of *NFIX* cause Marshall-Smith syndrome (MSS) (MIM: 602535), a more severe phenotype with severe intellectual disability, progressive dysostosis, respiratory difficulties,

[1]Institute of Human Genetics, University Hospital Magdeburg, Otto-von-Guericke University, Magdeburg 39120, Germany; [2]Queensland Brain Institute, The University of Queensland, Brisbane, QLD 4072, Australia; [3]Department of Clinical Genetics, Academic Medical Center, University of Amsterdam, Amsterdam 1105 AZ, the Netherlands; [4]INSERM U1183, Département de Génétique Médicale, Maladies Rares et Médecine Personnalisée, Génétique clinique, CHU Montpellier, Université Montpellier, Centre de référence anomalies du développement SORO, Montpellier 34295, France; [5]INSERM U1163, Laboratory of Embryology and Genetics of Congenital Malformations, Paris Descartes University, Sorbonne Paris Cité and Imagine Institute, Paris 75015, France; [6]Department of Medical Genetics, Haukeland University Hospital, Bergen 5021, Norway; [7]GeneDx, Gaithersburg, MD 20877, USA; [8]Department of Pediatrics (Genetics), University of Washington and Center for Integrative Brain Research, Seattle Children's Research Institute, Seattle, WA 98101, USA; [9]Manchester Centre for Genomic Medicine, Manchester Academic Health Science Centre, Central Manchester University Hospitals NHS Foundation Trust; Division of Evolution and Genomic Sciences School of Biological Sciences, and University of Manchester, Manchester M13 9WL, UK; [10]Boston Children's Hospital – The Feingold Center, Waltham, MA 02115, USA; [11]Division of Genetic Medicine, Seattle Children's Hospital, Seattle, WA 98105, USA; [12]The Faculty of Medicine Brisbane, The University of Queensland, Brisbane, QLD 4072, Australia; [13]UMR1231, Génétique des Anomalies du Développement, Université de Bourgogne, Dijon 21079, France; [14]Centre de Génétique et Centre de Référence Anomalies du Développement et Syndromes Malformatifs de l'Interrégion Est et FHU TRANSLAD, Centre Hospitalier Universitaire Dijon, Dijon 21079, France; [15]Department of Neurology, University of California, San Francisco, San Francisco, CA 94158, USA; [16]Service de Génétique, CHU de Caen - Hôpital Clémenceau, Caen Cedex 14000, France; [17]Service de Génétique Clinique, Hôpital Jeanne de Flandre, CHU Lille, Lille 59000, France; [18]Department of Clinical Genetics, Guy's Hospital, London SE1 9RT, UK; [19]Department of Pediatrics, Perelman School of Medicine at the University of Pennsylvania, Philadelphia, PA 19104, USA; [20]Division of Genetics, Department of Pediatrics, Children's Hospital of Philadelphia, Philadelphia, PA 19104, USA; [21]Department of genetics, Le Havre Hospital, 76600 Le Havre, France; [22]Department of Neurogenetics, Kennedy Krieger Institute, Baltimore, MD 21205, USA; [23]All Wales Genetics Laboratory, Institute of Medical Genetics, University Hospital of Wales, Cardiff CF14 4XW, UK; [24]Center for Human Genetics, University Hospital Leuven, KU Leuven, Leuven 3000, Belgium; [25]West of Scotland Genetics Service, Queen Elizabeth University Hospital, Glasgow G51 4TF, UK; [26]Medical Genetics Institute, Meir Medical Center, Kfar-Saba

(Affiliations continued on next page)

Samuel F. Huth,[2] Kosuke Izumi,[19,20] Bronwyn Kerr,[9] Elodie Lacaze,[21] Phillis Lakeman,[3] Sonal Mahida,[22] Ghayda M. Mirzaa,[8] Sian M. Morgan,[23] Catherine Nowak,[10] Hilde Peeters,[24] Florence Petit,[17] Daniela T. Pilz,[25] Jacques Puechberty,[4] Eyal Reinstein,[26,27] Jean-Baptiste Rivière,[13,14,28] Avni B. Santani,[29,30] Anouck Schneider,[4] Elliott H. Sherr,[15] Constance Smith-Hicks,[22] Ilse Wieland,[1] Elaine Zackai,[19] Xiaonan Zhao,[29] Richard M. Gronostajski,[31] Martin Zenker,[1,33,*] and Linda J. Richards[2,32,33]

and a characteristic facial dysmorphism, and is presumably a result of a dominant-negative mechanism.[24,27–29]

During normal brain development in mice, the expression patterns of *Nfia* and *Nfix* overlap with that of another family member, *Nfib*.[30–32] Knockout mice for any one of the three *Nfi* genes exhibit comparable brain defects, including dysgenesis of the corpus callosum and enlarged ventricles, which implies a common, but not redundant, function in brain development.[2,5,9,33,34] Considering the similar brain phenotypes of the *Nfia*, *Nfib*, and *Nfix* knockout mice, *NFIB* (MIM: 600728) is another strong candidate gene for intellectual disability and/or brain abnormalities in humans. To date, only a single 1.6 Mb deletion encompassing *NFIB* and five other genes has been reported in a subject with developmental delay and agenesis of the corpus callosum.[9,35] Here, we present a detailed clinical characterization of eight individuals with sequence variants in *NFIB* and ten individuals carrying overlapping microdeletions in the chromosomal region 9p23-p22.2, with the smallest region of overlap solely containing *NFIB*. Five individuals harbored nonsense mutations in *NFIB*, while three other individuals had *de novo* missense mutations within the DNA binding domain that cause a loss of function as demonstrated using a luciferase reporter assay. Furthermore, using a novel *Nfib* conditional knockout mouse model, we demonstrated that loss of *Nfib* results in an enlarged cortex, providing a direct link between a haploinsufficiency of *NFIB* in individuals and macrocephaly.

Subjects and Methods

Study Cohort

All 18 affected individuals were recruited independently through GeneMatcher or a network of collaborating clinicians and geneticists.[36] They presented for genetic evaluation due to developmental delay or intellectual disability.[37] Subjects' ages ranged from 3 to 33 years (median 8 years) at the time of assessment. Except for a pair of siblings and two mother-child pairs, all of the cases were sporadic and there were no instances of parental consanguinity. A summary of the clinical features of affected individuals is given in Tables 1 and 2. Facial features of eight individuals are shown in Figure 1, showing mild dysmorphic facial features. Detailed clinical information is provided in the Supplemental Note.

All genetic studies were done on genomic DNA extracted from blood samples. Array CGH/microarray-based molecular karyotyping was generally done on a clinical basis with informed consent given by the patient, parents, or a legal guardian according to the regulations of the respective countries. Whole-exome sequencing (WES) was performed in part of the cohort on a clinical basis with appropriate consent according to national regulations and in the other individuals on a research basis. All procedures that were done in a research environment had been approved by the responsible institutional committee on human experimentation. Moreover, signed consent for scientific evaluation and publication of genetic and clinical data (including photograph) was given by each participating individual or their legal guardians.

Molecular Karyotyping and Method of Confirmation

Molecular karyotyping was performed in subjects 8a, 9, and 13 using an Affymetrix genome-wide human SNP 6.0 array and in subject 8b using an Affymetrix genome-wide human SNP CytoScan HD array (Affymetrix, part of Thermo Fisher Scientific). Molecular karyotyping for subject 10a was carried out using a CytoSure ISCA v2 8x60k array and in subject 15 using a CytoSure ISCA v2 180K array (Oxford Gene Technology). In subject 11 molecular karyotyping was performed using the Agilent genome-wide SNP 60K array (Agilent Technologies). Molecular karyotyping in subject 12 was performed by the Illumina Infinium II HumanHap610 BeadChip (Illumina) and in subject 14 using the BlueGnome CytoChip (v1.1) BAC array (BlueGnome).

Experimental procedures were performed according to the manufacturer's instructions. Image data of the Affymetrix array were analyzed with the Affymetrix Genotyping console 3.0.1 and 4.1 and the Chromosome Analysis Suite v1.2 and v3.0. Image data of the OGT array were analyzed with the CytoSure Interpret software and of the BlueGnome array with the BlueGnome BlueFuse analyzing-software. For the Illumina array, analysis and CNV identification were done using the PennCNV software.

Results were interpreted using external and internal data resources. External resources include the Database of Genomic Variants (DGV),[38] DECIPHER,[39] ECARUCA,[40] ClinVar,[41] and OMIM.

The deletions in individuals 8a, 8b, 10a, 10b, and 13 were confirmed by multiplex-ligation dependent probe amplification (MLPA) using self-designed probes in exons 2, 4, and 11 of *NFIB* transcript ENST00000380953.5 (GenBank: NM_001190737.1) and in exon 1 of *NFIB* transcript ENST00000390934.8 (alternative

4428164, Israel; [27]Sackler Faculty of Medicine, Tel Aviv University, Tel Aviv 6997801, Israel; [28]Child Health and Human Development Program, Research Institute of the McGill University Health Centre, Montreal, QC H4A 3J1, Canada; [29]Division of Genomic Diagnostics, Children's Hospital of Philadelphia, Philadelphia, PA 19104, USA; [30]Department of Pathology and Laboratory Medicine, Perelman School of Medicine, University of Pennsylvania, Philadelphia, PA 19104, USA; [31]Department of Biochemistry, Program in Genetics, Genomics and Bioinformatics, Center of Excellence in Bioinformatics and Life Sciences, State University of New York at Buffalo, Buffalo, NY 14203, USA; [32]School of Biomedical Sciences, The Faculty of Medicine Brisbane, The University of Queensland, Brisbane, QLD 4072, Australia
[33]These authors contributed equally to this work
*Correspondence: j.bunt@uq.edu.au (J.B.), martin.zenker@med.ovgu.de (M.Z.)
https://doi.org/10.1016/j.ajhg.2018.10.006.

Table 1. Clinical Features in Individuals with NFIB Haploinsufficiency (Nucleotide Variations)

Subject	P1	P2	P3	P4	P5	P6a	P6b	P7
NFIB variant	p.Arg37*	p.Arg89*	p.Lys114Thr	p.Lys126Glu	p.Leu132Pro	p.Asn254*	p.Asn254*	p.Ile355Serfs*48
Inheritance	*de novo*	father unavailable	father unavailable	*de novo*	*de novo*	*de novo*	maternally inherited	*de novo*
Sex	M	M	M	M	M	F	M	F
Age at last examination	16 y	7 y	8 y	32 y	7 y	33 y	7 y	3 y
Prenatal Growth								
Birth weight (g) (SD)	2,750 (−1.30 SD; 10th)	4,000 (+0.89 SD; 81th)	2,495 (−1.70 SD; 4th)	3,080 (−0.77 SD; 22th)	3,280 (−0.45 SD; 33th)	2,960 (−0.89 SD; 19th)	3,900 (+0.69 SD; 75th)	3,020 (−0.77 SD; 22th)
Body length at birth (cm) (SD)	ND	ND	ND	50 (−0.06 SD; 48th)	52 (+0.70 SD; 76th)	ND	ND	48 (−0.81 SD; 21th)
OFC (cm) (centile)	ND	ND	ND	39.5 (+2.2 SD; 99th)	33 (−1.27 SD; 10th)	ND	ND	37 (+1.22 SD; 89th)
Postnatal Growth								
Height (cm) (SD)	173 (+0.20 SD; 58th)	124.9 (+0.58 SD; 72th)	137 (+2.80 SD; > 99th)	192.5 (+2.25 SD; 99th)	127 (+0.93 SD; 83th)	ND	ND	95.8 (+0.28 SD; 61th)
Weight (kg)	56 (−0.42 SD; 34th)	23 (−0.02 SD; 49th)	43.6 (+4.17 SD; >99th)	65 (−0.49 SD; 31th)	22.4 (−0.25 SD; 40th)	ND	ND	14.3 (+0.20 SD; 58th)
OFC (cm) (SD)	60.5 (+3.76 SD; >99th)	57.2 (+3.94 SD; >99th)	58 (+5.17 SD; >99th)	63 (+5.52 SD; >99th)	55 (+2.17 SD; 99th)	ND	ND	55 (+4.72 SD; >99th)
Neurodevelopmental Characteristics								
Muscular hypotonia	ND	Y	N	Y	Y	N	Y	Y
Motor delay	Y	N	Y	Y	Y	N	Y	Y
Speech delay	Y	Y	Y	Y	Y	Y	Y	Y
Intellectual disability	borderline	mild-moderate	mild-moderate	mild-moderate	borderline, developmental coordination disorder	mild	mild	mild
Attention deficit	N	Y	N	N	Y	NA	NA	N
Behavioral anomalies	short temper at younger age, problems with falling asleep	impulsivity	aggression, hyperactivity, impulsivity, autism	anxiety	autism, anxiety	NA	NA	N
Seizures	N	N	N	N	N	N	N	N
Neurological deficits	N	N	N	N	headaches	ND	ND	N

(*Continued on next page*)

Table 1. ***Continued***

Subject	P1	P2	P3	P4	P5	P6a	P6b	P7
Brain MRI Findings								
Corpus callosum anomaly	agenesis	mild thinning	N	N	partial hypoplasia	ND	ND	N
Ventriculomegaly	ND	N	N	N	N	ND	ND	Y
Other	ND	mildly infolded perisylvian regions likely due to thin white matter; mild cerebellar tonsillar ectopia	arachnoid cyst	cyst of septum pellucidum; diffuse cerebral atrophy; dorsal meningocele	ND	ND	ND	two small nodules of gray matter heterotopia along the frontal horns of the lateral ventricles; subtle irregularity and thickening along the posterior perisylvian cortex, right greater than left, which raises the possibility of polymicrogyria
Internal Malformations								
Genitourinary system	N	N	N	right cryptorchidism	N	N	N	N
Gastrointestinal system	N	N	N	N	N	N	N	N
Heart	N	N	N	N	N	N	N	innocent murmur
Other malformations	N	N		N	N	N	N	ND

Abbreviations: Y, trait present; N, trait absent; ND, not determined; NA, not applicable; ID, intellectual disability; SD, standard deviation; gw, weeks of gestation.

Table 2. Clinical Features in Indifviduals with NFIB Haploinsufficiency (Deletions)

Subject	P8a	P8b	P9	P10a	P10b	P11	P12	P13	P14	P15	Summary All Subjects
Aberration	9p23p22.3 (14098659_ 14324147)x1	9p23p22.3 (14098659_ 14324147)x1	9p22.3p23 (14102175_ 14386038)x1	9p23p22.3 (13974415_ 14286259)x1	9p23p22.3 (13974415_ 14286259)x1	9p23p22.3 (13106806_ 14639971)x1	9p23p22.3 (13034407_ 14653394)x1	9p23p22.2 (14178768_ 16619009)x1	9p23p22.2 (13563537_ 18491752)x1	9p23p22.2 (13739630_ 18023839)x1	
Deletion size	225 kb	225 kb	284 kb	312 kb	312 kb	1.5 Mb	1.6 Mb	2.4 Mb	4.9 Mb	4.3 Mb	
Inheritance	familial	familial	*de novo*	*de novo*	maternally inherited	*de novo*	unknown	*de novo*	*de novo*	*de novo*	
Sex	F	F	M	F	F	M	M	F	M	F	
Age at last examination	6 y	8 y	7 y	20 y	3 y 5 m	8 y 4 m	21 y	7 y 10 m	10 y	17 y	
Prenatal Growth >2 SDS											
Birth weight (g) (SD)	ND	3,470 (−0.1 SD; 54th)	3,500 (−0.10 SD; 46th)	4,400 (+2.13 SD; 98th)	3,400 (−0.05 SD;48th)	2,750 (−1.30 SD; 10th)	ND	4,030 (+1.32 SD; 91th)	3,200 (−0.58 SD; 28th)	3,370 (−0.11 SD; 46th)	1/16
Body length at birth (cm) (SD)	ND	ND	50 (−0.06 SD; 48th)	58 (+3.1 SD; > 99th)	ND	49 (−0.44 SD; 33th)	ND	56 (+2.38 SD; 99th)	49 (−0.44 SD; 33th)	ND	2/7
OFC (cm) (centile)	ND	ND	37 (+0.68 SD; 75th)	39 (+1.92 SD; 97th)	37 (+1.22 SD; 89th)	34 (−0.83 SD; 20th)	ND	37 (+1.22 SD; 89th)	ND	ND	1/8
Postnatal Growth >2 SDS											
Height (cm) (SD)	122.6 (+1.46 SD; 93th)	131 (+0.56 SD; 71th)	131 (+1.70 SD; 96th)	165 (+0.27 SD; 61th)	92 (−0.68 SD; 25th)	131.5 (+0.62 SD; 73th)	177.8 (−0.17 SD; 57th)	137 (+2.68 SD; >99th)	144 (+0.80 SD; 79th)	(75 centile)	3/16
Weight (kg)	26.2 (+1.32 SD; 91th)	28.9 (+0.49 SD; 69th)	22 (−0.41 SD; 34th)	68.5 (+0.68 SD; 75th)	18.9 (+2.36 SD; 99th)	25.5 (−0.04 SD; 48th)	ND	43.9 (+3.82 SD; >99th)	41 (+0.99 SD; 84th)	(50–75 centile)	3/15
OFC (cm) (SD)	55.6 (+3.35 SD; >99th)	55.2 (+2.71 SD; >99th)	55 (+2.17 SD; 99th)	61 (+6.01; >99th)	55.5 (+4.60 SD; >99th)	52.5 (+0.15 SD; 56th)	61.5 (+4.46 SD; >99th)	57 (+4.39 SD; >99th)	54.5 (+1.19 SD; 88th)	(50–75 centile)	13/16
Neurodevelopmental Characteristics											
Muscular hypotonia	N	N	Y	Y	Y	N	N	Y	Y	Y	11/17
Motor delay	ND	ND	Y	Y	Y	N	Y	N	Y	N	11/16
Speech delay	Y	Y	Y	Y	Y	Y	Y	Y	Y	Y	18/18
Intellectual disability	learning disability (not formally tested)	borderline mild ID	learning disability	mild	mild	mild	learning disability	mild	mild	learning disability	18/18
Attention deficit	Y	Y	Y	Y	NA	Y	Y	Y	Y	Y	11/15

(*Continued on next page*)

Table 2. ***Continued***

Subject	P8a	P8b	P9	P10a	P10b	P11	P12	P13	P14	P15	Summary All Subjects
Behavioral anomalies	reactive attachment disorder, passive, pleasing	autistic features, social difficulties	N	short temper	NA	anxiety, hetero-agressivity	ASD, impulse control problems, trouble gauging emotions	Y	ASD and psychotic episodes	Y	13/15
Seizures	N	N	N	N	N	N	N	N	N	N	0/18
Neurological deficits	N	N	N	ND	ND	N	insensitivity to pain, temperature dysregulation	N	N	N	2/14
Brain MRI Findings											**9/11**
Corpus callosum anomaly	ND	N	N	ND	ND	ND	complete agenesis	complete agenesis	N	ND	5/11
Ventriculomegaly	ND	N	N	ND	ND	ND	Y	N	N	ND	2/11
Other	ND	slight asymmetric hemispheres	NA	ND	ND	ND	moderately decreased white matter volume; bilateral probst bundles	mildely decreased white matter volume	NA	ND	7/11
Internal Malformations											**7/17**
Genitourinary system	N	N	N	N	N	ND	N	N	cryptorchidism	N	2/17
Gastrointestinal system	N	N	N	N	N	ND	N	N	N	N	0/17
Heart	small VSD	narrow pulmonary artery, normalized at 2 y	N	N	PDA	ND	N	N	N	bicuspid aortic valve	5/17
Other malformations	N	N	N	N	N	NA	N	N	N	N	0/17

Abbreviations: Y, trait present; N, trait absent; ND, not determined; NA, not applicable; ID, intellectual disability; SD, standard deviation; gw, weeks of gestation.

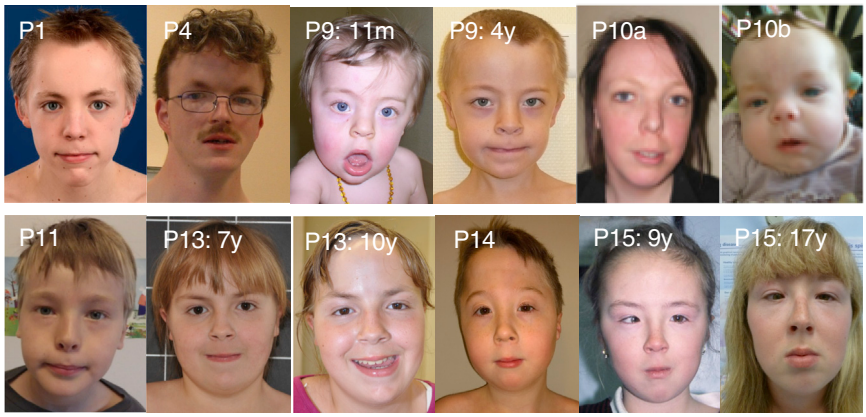

Figure 1. Clinical Features of Individuals with *NFIB* Haploinsufficiency
Craniofacial phenotype of individuals P1, P4, P9, P10a, P10b, P11, P13, P14, and P15. The pictures show individual P9 at the age of 11 months and at the age of 4. Individual P13 is represented at the ages of 7 and 10 years, while P15 is represented at the ages of 9 and 17 years. Note the long face with the high forehead, sparse eyebrows, down-slanting palpebral fissures and mild blepharophimosis, a narrow nasal bridge, anteverted nares, and a long and smooth philtrum.

first exon; GenBank: NM_001190738.1) (Figure S1). In subject 9 validation was performed by FISH analyses with a mix of locus-specific probes. The amplification of the sequence overlapping the deletion breakpoints in the subject was achieved by long-range PCR. In individuals 11 and 12 validation was performed by qPCR.

Sequencing and Filtering of Variants

Whole-exome capture and sequencing were performed in subjects 1, 2, 3, and 4 (singletons), 6a/6b (child-parent pair), and 5 and 7 (child-parent trios) using the SeqCap EZ MedExome (Roche NimbleGen), Agilent SureSelect Human All Exon V4/V5, Agilent Clinical Research Exome Kit (Agilent Technologies), or Nextera Rapid Capture Exome (Illumina). Libraries were sequenced on an Illumina HiSeq (2000, 2500, or 4000) according to the manufacture's recommendation for 75 bp, 100 bp, or 125 bp paired-end reads, respectively. Sequence reads were aligned to the human reference genome (hg19) using different versions of the Burrows-Wheeler Alignment software (BWA v.0.5.8-v.0.6.2 to BWA-Mem v.0.7.5-8). The Genome Analysis toolkit software package (GATK v.1.6.9 to v.2.6-4) or SAMtools v.0.1.18.10 were used for base quality score recalibration, indel realignment, and variant discovery (both single-nucleotide variants and indels). Common variants (defined as variants with >1% frequency in dbSNP, 1000 Genomes Browser, NHLBI Exome Sequencing Project Exome Variant Server, and/or the Exome Aggregation Consortium ExAC Browser) were excluded. *De novo*, homozygous, compound heterozygous, heterozygous, or X-linked variants (on the basis of inheritance pattern based on the family structure and reported phenotype) present in exons or at exon/intron boundaries (±6 nt in the intron) were examined. *In silico* analysis of the sequence variants was performed using the open access software PredictSNP2,[42] Mutation Taster,[43] PROVEAN/SIFT,[44] and PolyPhen-2.[45] Sequence alterations are reported according to the Human Genome Variation Society (HGVS) nomenclature guidelines. All relevant variants identified by NGS were validated by conventional Sanger sequencing in forward and reverse direction (Figure S1).

Generation and Validation of Mutant NFIB Expression Constructs for Luciferase Assays

The *NFIB* missense single-nucleotide variations identified in individuals with ID were cloned into the pCAG-*Nfib*-IRES-GFP plasmid containing a HA-tagged mouse *Nfib* coding sequence (CCDS38790.1).[46] The mouse NFIB protein is 99% identical to the 420 aa human protein encoded by isoform 3 (GenBank: NM_005596.3/CCDS6474.1), with only two amino acid substitutions that were not located near any of the mutated sites. Primers recognizing the plasmid backbone (Table S1) were used in combination with reciprocal primers containing the missense variant to generate two fragments that were amplified using the Phusion High-Fidelity DNA Polymerase (New England Biolabs) and pCAG-*Nfib*-IRES-GFP as a template. The two fragments were annealed and then amplified using plasmid-specific primers to generate a full-length *Nfib* insert containing the missense mutation. Mutant *Nfib* inserts were digested with NotI (New England Biolabs), ligated into the NotI-digested pCAG-*Nfib*-IRES-GFP backbone, and verified by Sanger sequencing. Protein size and expression were validated by western blots of transfected cells.

Dual-Luciferase Reporter Assays

Neuro-2A[47] or U251[48] cells were seeded into a 96- or 48-well plate 24 hr prior to transfection at a density of 30%–50% and maintained in DMEM (Sigma-Aldrich) supplemented with 10% v/v fetal bovine serum (SAFC Biosciences, part of Sigma-Aldrich). The pGFAPp-Luc firefly luciferase reporter construct[49] was co-transfected with either the empty pCAG-IRES-GFP or the wild-type or mutant pCAG-*Nfib*-IRES-GFP construct into seeded cells using FuGENE 6 transfection reagent (Promega). The pNL1.1.TK NanoLuc luciferase vector (Promega) was co-transfected with all transfections as an internal control to normalize for transfection efficiency. Luciferase activity was assayed 48 hr after transfection using the Nano-Glo Dual-Luciferase Reporter Assay system (Promega) and the POLARstar OPTIMA plate reader (BMG Labtech, part of Thermo Fisher Scientific). Statistical significance was determined using the Student's t test.

Mouse Brain Collection and Analyses

All mice were housed and handled in accordance with the National Health and Medical Research Council's Australian Code of Practice for the Care and Use of Animals for Scientific Purposes and with approval from the University of Queensland Animal Ethics Committee. The FLR-flanked neomycin cassette was removed in the *Nfib* conditional strain Nfib^{tm2Rmg} to generate Nfib$^{tm2.1Rmg}$.[50] Nfib$^{tm2.1Rmg}$;Gt(ROSA)26Sor$^{tm14(CAG-tdTomato)Hze}$;Emx1-iCre[51,52] mice, henceforth referred to as *Nfib*^{flxdn};*tdTom*;Emx1iCre, were housed at the Queensland Brain Institute animal facility on a 12 hr dark/light cycle with water and food provided *ad libitum*. *Nfib*^{flxdn};*tdTom*;Emx1iCre animals were bred to generate progeny that were all homozygous for both *Nfib*^{flxdn} and *tdTom* and either negative (wild-type; WT) or positive (conditional

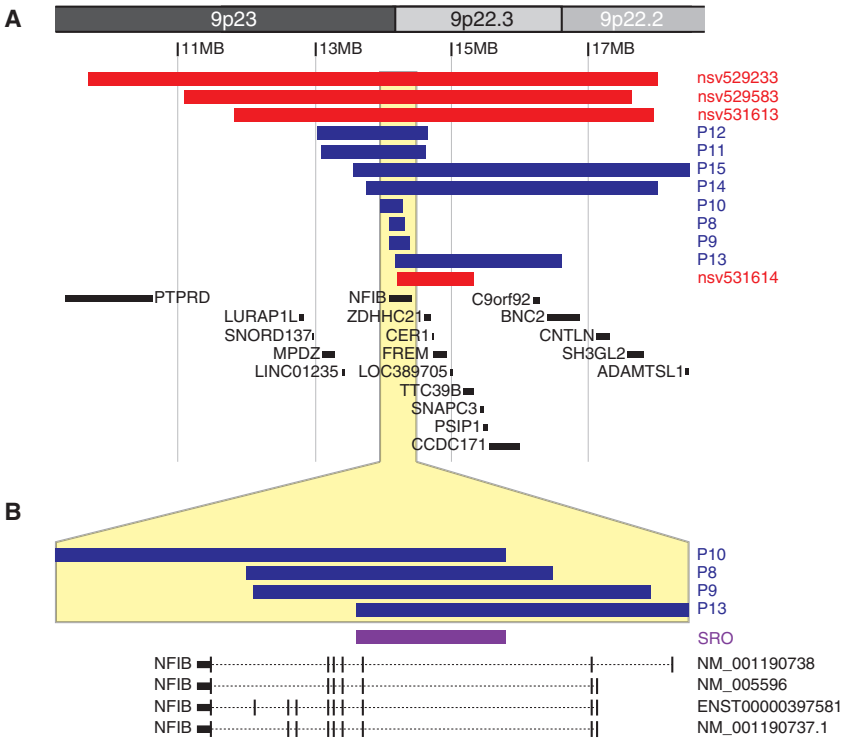

Figure 2. The Smallest Region of Overlap in 9p23-p22 Deletions within *NFIB*

(A and B) Graphical depiction of the deletions overlapping with *NFIB* on chromosome 9p23-p22 detected in individuals P8–P15 (blue). In red, four additional cases from the ClinVar database are depicted. The smallest region of overlap, depicted in purple in (B), contains only exon 3 of *NFIB*. Adapted from UCSC Genome Browser hg19.

knockout; cKO) for Emx1iCre. All animals were genotyped by the Australian Equine Genetics Research Centre (AEGRC; University of Queensland, Brisbane, QLD, Australia).

Animals anesthetized with an intraperitoneal injection of sodium pentobarbitone (Lethabarb; Virbac; 185 mg/kg body weight) were transcardially perfused with saline, followed by 4% w/v paraformaldehyde solution, as previously described.[53] After 5–7 days of post-fixation at 4°C–7°C, the brains were dissected from the skull and measured using calipers. Magnetic resonance images were acquired at the Centre for Advance Imaging at the University of Queensland using a 16.4 Tesla vertical bore, small animal MRI system (Bruker Biospin; ParaVision v5.0). Acquisition, brain measurements, and tractography are described in detail in the Supplemental Methods. In short, brain orientation was standardized between mice, and the lengths and cross-sectional areas of specific brain structures were measured in either the mid-sagittal plane or the coronal plane at Bregma level −2.18 mm. All analyses were normalized to total brain height (dorso-ventral size) or length (rostro-caudal size) to account for size variations between individual mice. Probabilistic tractography was performed to detect cortical connectivity and topographic organization of the corpus callosum.[54,55] The structural MR image for each mouse brain was divided into 20 segments via the multi-atlas segmentation tool provided by Advanced Normalization Tools (v 2.2.0, stnava). Nine hand parcellated mouse brain atlases from the Magnetic Resonance Microimaging Neurological Atlas formed the basis of the multi-atlas segmentation.[56] The segmented images were analyzed in MATLAB (v R2015b, MathWorks) to determine the number of voxels within the bounds of each segment and calculate their total volume for each mouse brain. For detailed information, see Supplemental Methods.

For histological analyses, dissected brains were embedded in 3%–3.5% Difco Noble agar (Becton, Dickinson and Company) in distilled water and sectioned coronally at 50 μm on a vibratome (Leica). The sections were then mounted onto SuperfrostPlus slides (Menzel-Gläser) and dried at room temperature until fully adherent. Sections were incubated in 4′,6-diamidino-2-phenylindole (DAPI) (1:1,000; Thermo Fisher Scientific) in 0.2% Triton X-100 in PBS for 5 min. The sections were then washed for 3 × 20 min with PBS and coverslipped using ProLong Gold anti-fade reagent (Thermo Fisher Scientific). Fluorescence imaging was performed with a Metafer VSlide Scanner fitted with a Zeiss Axio Imager Z2 (Metasystems). Images were pseudocolored, cropped, sized, and enhanced for contrast and brightness with Imaris 8.2.1 software (Bitplane), ImageJ (NIH), and Illustrator (Adobe Systems). All relevant measurements were made using ImageJ.

For animals of postnatal day (P) 25 or older, only females were included to exclude sex-based size differences. For each stage, 3–8 cKO and WT littermates were measured. Significance was determined using a one-way ANOVA.

Results

Molecular Karyotyping Identifies Disruption of *NFIB* as the Common Consequence of 9p23-p22.2 Microdeletions

We identified overlapping deletions in the 9p23-p22.2 chromosomal region in ten individuals with mild ID and other behavioral features (Table 2 and Supplemental Note).[37] These included two siblings (P8a and 8b), a mother and daughter (P10a and 10b), and six other unrelated individuals (P9, P11–P15) with deletions ranging in size from 225 kb to 4.9 Mb (Figure 2A). Individual 12 was previously reported without a full clinical description.[9,35]

The deletions in individuals 10a, 10b, and 13 delineate the smallest region of overlap, comprising a genomic segment of 107 kb (chr9: 14,178,768–14,286,259; hg19) that encompasses only *NFIB* (Figure 2B). The breakpoints of the deletions are non-recurrent. Three individuals (P8a, 8b, 9) presented with intragenic deletions affecting only *NFIB*. By MLPA analysis, using self-designed probes, we confirmed that the affected siblings 8a and 8b harbored an intragenic deletion affecting exons 1–10 of the *NFIB* transcript ENST00000380953.5 (Figure S1). Parental samples were not available to determine whether or not this

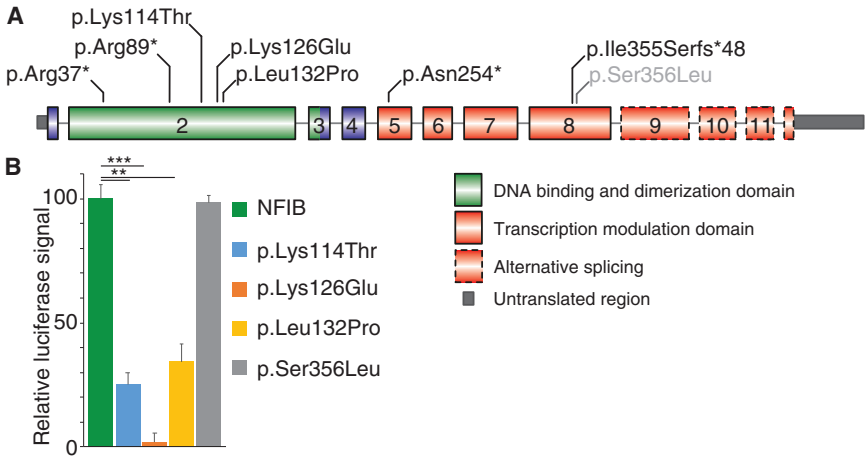

Figure 3. Sequence Varations Identified in *NFIB*

(A) Schematic representation of the identified sequence variations in *NFIB* in individuals P1–7 (black) and in the fetal case (gray), based on GenBank: NM_001190737.1 (ENST00000380953.5). (B) The missense variants found in individuals 3, 4, and 5 were cloned into an NFIB overexpression construct. Using the *GFAP*-promoter reporter construct in a dual-luciferase assay in U251 and Neuro-2A cells, their ability to induce promoter activity was tested. The data represent one of these experiments with the relative luciferase signal increase to the vector control normalized to wild-type NFIB. All three missense variants—p.Lys114Thr, p.Lys126Glu, and p.Leu132Pro—resulted in significantly less promoter activity, while another missense variant (p.Ser356Leu) did not alter activity. The data depicted are representative of three independent experiments, each consisting of 4–6 technical replicates. Error bars represent standard error and the significance was determined by one-way ANOVA. ***$p < 0.0005$, **$p < 0.005$.

deletion was inherited. The *de novo* 284 kb deletion in individual 9 likewise encompassed exons 1 to 10 of *NFIB*, but the deletion breakpoints differed. In individuals 10a and 10b, the results of MLPA analysis indicated that the proximal deletion breakpoint was located within intron 2, thus mapping the deletion to exons 3 to 11 of *NFIB*. Individual 10a inherited the deletion, which originated *de novo* in her affected mother, 10b. In four other simplex case subjects, the deletion was confirmed to be *de novo*, while parental samples were not available for one individual (P12).

Exome Sequencing Identifies *De Novo* Missense and Nonsense Variants in *NFIB*

In eight individuals from seven families with ID, who had previous molecular karyotyping with normal results, WES was performed and revealed sequence variants in *NFIB* (GenBank: NM_001190737.1; Figure 3A). These included four variants predicting premature termination codons: c.109C>T (p.Arg37*) (P1), c.265C>T (p.Arg89*) (P2), c.758_759dupTG (p.Asn254*) (P6a and b), and c.1063_1076del (p.Ile355Serfs*48) (P7). The other three observed variants were missense changes predicted to affect highly conserved amino acid residues within the DNA-binding and dimerization domain of NFIB: c.341A>C (p.Lys114Thr) (P3), c.376A>G (p.Lys126Glu) (P4), and c.395T>C (p.Leu132Pro) (P5). None of these variants were present in public databases (dbSNP, 1000 Genomes Browser, NHLBI Exome Sequencing Project Exome Variant Server, the Exome Aggregation Consortium ExAC Browser). Parental DNA studies confirmed that variants were *de novo* in individuals 1, 4, 5, and 7 as well as in individual 6a who transmitted the variant to her similarly affected son, individual 6b. Parental samples were not available for individuals 2 and 3.

Additionally, targeted exome sequencing detected the *NFIB* variant c.1067C>T (p.Ser356Leu) in a 29-week fetus with hypoplasia of the corpus callosum and pulmonary sequestration.[57] This variant was also present in the mother, who had no physical abnormalities and normal intellect (Supplemental Note).

To predict the impact of these variants on NFIB function, we performed *in silico* analyses. Based on PredictSNP2, the variants were classified as damaging (Table S2).[42] For the four variants that introduce premature stop codons, a truncated protein is predicted, which removes (part of) the transactivation domain. In addition, these variants might contribute to mRNA clearing via nonsense-mediated RNA decay, as shown previously for *NFIX*.[29] Notably, a C-terminally truncated protein with strongly reduced transcriptional ability was previously reported in humans.[58] The three observed missense variants were consistently predicted to affect protein function by all employed prediction programs.

Functional Analyses Reveal Loss of Function of *De Novo* Missense Variants in *NFIB*

To further investigate the functional impact of the missense variants p.Lys114Thr, p.Lys126Glu, p.Leu132Pro, and p.Ser356Leu, these sequence variants were cloned into an NFIB expression construct.[46,59] We then analyzed their ability to activate the human *GFAP* promoter,[49] a well-established transcriptional target of NFIB, to determine whether mutant NFIB displays a disrupted function.[5,7,9,60] In a luciferase reporter assay in which luciferase is driven from the *GFAP* promoter, wild-type NFIB increased luciferase activation, as previously published (Figure 3B).[9] When the three mutated proteins were tested in this assay, we observed that all three resulted in a significant reduction in luciferase activity compared to the wild-type protein. In contrast, the missense variant p.Ser356Leu displayed luciferase activity similar to the wild-type protein. Based on these results, we confirmed that the p.Lys114Thr, p.Lys126Glu, and p.Leu132Pro missense variants confer loss of function,

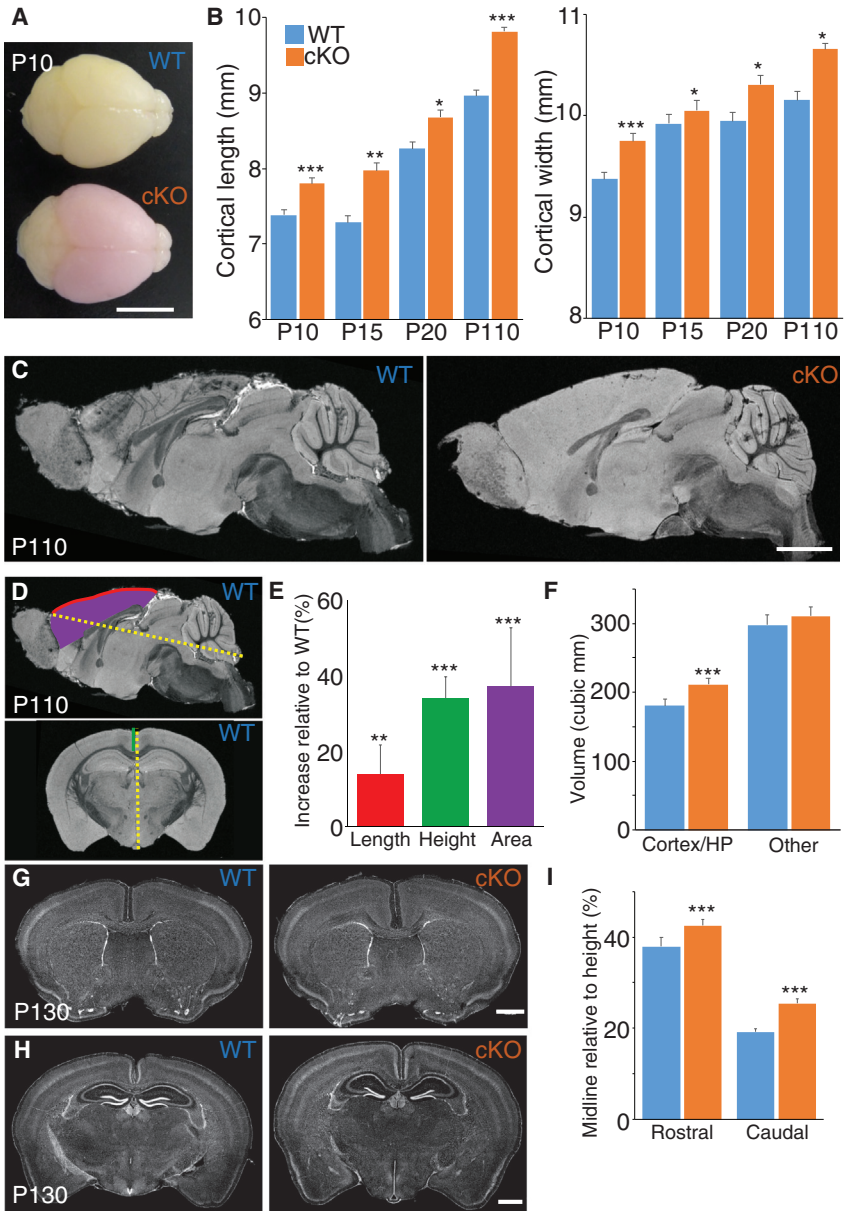

Figure 4. Cortical-Specific Knockout of *Nfib* Results in an Enlargement of the Cortex

(A) Representative brains of homozygous *Nfib* conditional littermates with Cre (conditional knockout; cKO) and without Cre (wild-type; WT) at postnatal day (P) 10. The cKO brain expresses tdTomato red fluorescent protein as a reporter for Cre-mediated *Nfib* knockout. Scale bar is 5 mm.

(B) Based on measurements of dissected brains from cKO and WT littermates, the cortical length and width were significantly increased in cKO compared to WT animals at P10, P15, P25, and P110. Error bars represent standard error and the significance was determined by a one-way ANOVA. P10, n = 8 for both groups; P15, n = 5 and 6; P25, n = 3 and 5; P110, n = 8 and 4 for WT and cKO, respectively. ***p < 0.0005, **p < 0.005, *p < 0.05.

(C) Fast low-angle shot (FLASH) MRI images of the same P110 animals measured in (B) revealed no major changes of the overall brain structure of cKO brains compared to WT littermates. Scale bar is 2 mm.

(D and E) The overall length (red line) and surface area (purple) of the cortex normalized to the overall brain length (yellow) was increased. Similarly, the height of the cortex at the midline (green line in coronal section), as measured from the corpus callosum to the caudal tip of the brain and normalized to the total height (yellow line in coronal section), was also increased. Significance was determined by Welch's corrected t test. n = 7 and 8. ***p < 0.0005, **p < 0.005.

(F) Based on MRI, the volumes of the cortex and hippocampus (HP) increased more than 16%, while the volume of the other brain structures only slightly increased. Significance was determined by Welch's corrected t test. n = 7 and 8. ***p < 0.0005.

(G and H) Histological analyses of independent brains at P130 confirmed no major structural changes, including in cortical lamination. Scale bar is 1 mm.

(I) Similar to the measurements in MRI images, the cortical height at the midline was increased. Significance was determined by Welch's corrected t test. P10, n = 4 and 6. ***p < 0.0005. All error bars represent standard deviation.

while the p.Ser356Leu variant showed no functional impact in this assay, consistent with the assumption that this maternally transmitted variant is likely non-pathogenic.

Nfib Deletion Results in Increased Cortical Size

In addition to mild ID, macrocephaly was observed in all individuals with *NFIB* sequence variants (P1–P7) and in individuals with haploinsufficiency due to deletions encompassing just *NFIB* (P8a–P10b; Table 2). In *Nfib* knockout mouse embryos, the perturbed development of the dorsal telencephalon has been shown to be associated with increased generation of progenitor cells.[5,7–9,61] This increase in progenitors may directly impact the overall size of the cortex and therefore head size. However, this has not been confirmed previously, because *Nfib* deletion in mice is perinatally lethal due to defects in lung maturation.[7]

To determine whether disruption of *NFIB* expression increases cortical size, we generated a dorsal telencephalon-specific *Nfib* conditional knockout model, *Nfib*^{flxdn}; *tdTom*;*Emx1*iCre, including a red fluorescent marker protein to indicate regions of Cre-recombination and *Nfib* deletion (Figure 4A).[50–52] Analyses of the size of the cortex of these mice at postnatal day 10, 15, 25, and 110 demonstrate that conditional knockout of *Nfib* in Cre-positive mice (cKO) resulted in a significant increase in cortical length and width (medio-lateral size) compared to their Cre-negative littermates (WT) at all ages (Figure 4B; one-way ANOVA).

To further determine whether *Nfib* deletion altered the overall structure of the cortex, fast low-angle shot (FLASH; Figure S2) and diffusion-weighted spin-echo magnetic resonance imaging (dMRI; Figures 4C and 4D)[54,55] as well as histological analyses (Figures 4G and 4H) were performed. No major structural changes were observed in the brain. Specific measurements on brain structures in MRI images and histological sections did reveal that the corpus callosum was slightly shorter and thinner in *Nfib* cKO animals (Figures 4C, 4G, and 4H), although these findings were not statistically significant.

The cortex was expanded in length (rostro-caudal dimension; Figure 4E) and height, when measuring from the corpus callosum to the caudal tip (Figures 4E and 4I). However, the overall radial thickness of the cortex and individual cortical layers were not altered compared to wild-type littermates. This suggests that the increased cortical size is mainly due to a lateral expansion, which is in line with the increased number of radial glia observed in *Nfib* knockout mice during early cortical development.[7,34,46]

Based on MRI, the overall brain volume of the cKO animals was almost 10% larger than that of their Cre-negative littermates. After segmentation of the brain in different regions,[56] the cortical and hippocampal volume contributed 70% of the total increase in volume (Figure 4F), while the increase of all other brain structures, including the cerebellum and thalamus, was not significant. Hence, these data suggest that the increased head circumference and macrocephaly identified in individuals with *NFIB* haploinsufficiency may correspond to megalencephaly secondary to lateral expansion of the cortex during fetal development.

Discussion

Here, we report overlapping heterozygous microdeletions in the chromosomal region 9p23-p22.2 and sequence variants affecting *NFIB* in individuals with a neurodevelopmental phenotype characterized by ID, macrocephaly, and other features. The pathogenic significance is supported by the confirmation of *de novo* occurrence in 9 out of 11 simplex case subjects, where parental samples were available. In three familial case subjects, the *NFIB* deletion or sequence variant segregated with the phenotype. Individual 10b inherited the deletion from her similarly affected mother, 10a, in which the deletion had occurred *de novo*. Similarly, individual 6b inherited the sequence variant from his affected mother. The affected siblings (subjects 8a and 8b) also likely inherited the deletion from an affected parent, but clinical details on the biological parents were insufficient and DNA samples were unavailable.

The entire region involved in the various 9p23-p22.2 deletions presented here encompasses 16 genes (chr9:13,106,806–18,491,752; Figure 2A), of which haploinsufficiency is predicted for five (*NFIB*, *ZDHHC21*, *PSIP1*, *BNC2*, *SH3GL2*).[62] However, since the smallest region of overlap contained only exon 3 of *NFIB* and because microdeletions in individuals 8a, 8b, and 9 are intragenic deletions of *NFIB* (Figure 2B), *NFIB* is the only gene shared between the case subjects. The pLI score (probability of LoF intolerance) for *NFIB* is 0.99, indicating a very high likelihood for haploinsufficiency of this gene.[63]

The role of *NFIB* haploinsufficiency as the causative event is further supported by the identification of seven sequence variants of *NFIB* in six simplex and one familial case subject with similar phenotypes. Four of the observed variants create premature termination codons in exons 2, 5, and 8, respectively, thus plausibly suggesting loss of function of the mutant allele. The three missense sequence variations, p.Lys114Thr, p.Lys126Glu, and p.Leu132Pro, were predicted as also likely damaging mutations *in silico* (Table S2), and we were able to confirm the impaired function of mutant proteins *in vitro* by demonstrating a severe reduction of transcriptional activity compared to wild-type NFIB. In contrast, the missense variant p.Ser356Leu, detected by WES in a fetus with brain anomalies but also in the unaffected mother and predicted damaging *in silico*, did not demonstrate a loss of function in our *in vitro* test assay. These findings can be regarded as a confirmation of the validity of this assay to detect functionally defective NFIB proteins with respect to DNA binding and transcription activation.

Clinical Presentation

All 18 individuals with haploinsufficiency of *NFIB* presented with mild intellectual disability or learning disability and speech delay. Motor delay (12/16) and muscular hypotonia (11/17) were also commonly reported (Tables 1 and 2). *NFIB* deletion and sequence variant carriers also showed attention deficit disorder (11/14) and variable behavioral anomalies including autistic behavior, anxiety, psychotic episodes, and aggression. Furthermore, 13/16 individuals presented with macrocephaly ($>97^{th}$ centile; Figures S3A and S3B).

Variable structural brain anomalies were reported based on brain imaging (9/11), including dysgenesis of the corpus callosum as the most common, albeit not consistent, finding (5/11) (Tables 1 and 2 and Figure S4). As brain imaging was not available in some cases, and since high-quality imaging and specific analysis may be required to properly identify corresponding anomalies in humans, the full spectrum of structural brain anomalies in the affected individuals remains to be analyzed in detail.

Although striking craniofacial anomalies were not part of the phenotype, affected individuals did share some minor facial dysmorphic features including a long face with high forehead, sparse eyebrows, down-slanting palpebral fissures and blepharophimosis, a narrow nasal bridge, anteverted nares, a long and smooth philtrum, and small ears (Figure 1). No major malformations in other organ systems were recorded, although five individuals had minor heart defects and two male individuals had cryptorchidism. No

lung defects have been reported in any of the individuals with pathogenic *NFIB* changes, contrasting with the frequency of lung maturation defects in both heterozygous and homozygous knockout mouse embryos.[7,64] Whether this reflects perinatal lethality, partial retention of protein function in sequence variants, or developmental differences between species remains unclear.

Despite the varying size of the deletions encompassing *NFIB*, the severity of cognitive impairment was similar in all individuals with 9p23-p22.2 microdeletions and was comparable to that seen in point mutation cases. However, individuals with larger deletions displayed a slightly different clinical presentation. For instance, facial anomalies were more pronounced in these individuals (Figure 1). It is therefore possible that other dosage-sensitive genes in the larger-sized deletions might be contributing to the expanded phenotype of these individuals (Figure 2A). Similarly, these other genes could mitigate the macrocephaly, as the three individuals without macrocephaly had large deletions involving multiple genes.

Developmental Origin of Defects in NFIB Deficiency

Much of our understanding about the function of NFIB is based on analyses of embryos from *Nfib* knockout mouse models. These studies have revealed the importance of NFIB for normal cortical development. *Nfib* knockout embryos display multiple defects, including agenesis of the corpus callosum, enlarged ventricles, and hippocampal anomalies.[5,7,9,46,61] On a cellular level, cortical progenitor cells remain self-renewing for longer in *Nfib* knockout mice, and neurogenesis and gliogenesis are delayed.[8,34] However, it has not previously been possible to study the postnatal structural and functional consequences of this developmental brain phenotype as these animals are not viable due to lung failure.[7,64]

In this study, we use a conditional knockout mouse model with *Nfib* deletion localized to the dorsal telencephalon. As a consequence, homozygous conditional knockout animals remain viable postnatally. These animals displayed an isolated increase in cortical size without other structural brain defects. Overall, cortical lamination and interhemispheric wiring is similar to those of wild-type animals, which is consistent with observations in complete null embryos of the constitutive knockout model.[8] Although further analysis is required, the increased radial glial population due to *Nfib* deletion in mice appears to be the likely cause of the observed increase in cortical size.[34,46] Developmentally, this increase results in ventricular enlargement, especially near the midline, where NFIB expression is higher than in lateral regions of the cortex.[7,34]

In contrast to the previous constitutive *Nfib* knockout model, which displays fully penetrant complete agenesis of the corpus callosum and aberrant fiber tracts,[5,7,9] homozygous conditional knockout mice have a corpus callosum. We recently identified that complete agenesis in *Nfib* knockout mice is caused by a defect in midline glial development that disrupts interhemispheric midline remodeling.[65] In heterozygous embryos of the constitutive *Nfib* knockout model, complete callosal agenesis has not been observed, although sporadically embryos displayed milder forms of callosal dysgenesis.[7] The corpus callosum in homozygous conditional knockout mice is slightly shorter and thinner (Figures 4C and 4E) but exhibits no interhemispheric wiring defects. In these conditional knockout mice, *Nfib* was not deleted in the midline glia, therefore permitting midline fusion and the formation of the corpus callosum.[9,35]

Overlapping Function of NFIA, NFIB, and NFIX

In mice, *Nfia*, *Nfib*, and *Nfix* display a very similar expression pattern during early brain development, although their expression becomes more distinct at later ages.[30,32,66] Each of the individual *Nfi* knockout mice display comparable cortical defects, particularly for *Nfia* and *Nfib* knockout embryos.[1,2,5–9,46,61] In this context, all three family members function non-redundantly and additively.[34,67] Hence, the number of *Nfi* alleles corresponds with the severity of the observed cortical phenotype, such that *Nfib* homozygous knockout and *Nfia*;*Nfib* double heterozygous knockout mice display similar severity of phenotypes.[34,67] This overlap in biological function may explain the similarities between the individuals with *NFIB* haploinsufficiency described here and those with *NFIA* or *NFIX* haploinsufficiency (Figure S3C).

The NFI proteins share a highly homologous N-terminal DNA-binding and dimerization domain, mainly encoded by exon 2,[3] and disease-causing mutations may occur in homologous amino acids between family members. Indeed, missense variants, corresponding to the p.Lys114Thr and p.Lys126Glu observed in subjects 3 and 4, has been recently reported in an individual with Malan syndrome in the respective codon of *NFIX* p.Lys113Glu, p.Lys125Glu, and p.Lys125Gln.[21,68] The region surrounding these lysines could be important for NFI function, as we observed a p.Leu132Pro missense change in *NFIB* in subject 5, while p.Arg115Trp, p.Arg116Gly, p.Arg116Gln, p.Arg116Prf, p.Arg121Pro, and p.Arg128Gln have been reported in *NFIX*.[68–71]

Association of NFIB with Intellectual Disability and Other Neurological Disease

More cases with mild intellectual disability and variable behavioral anomalies may potentially be linked to *NFIB* loss or altered expression. In the ClinVar database,[72] four entries with deletions overlapping *NFIB* (dbVar: nsv529583, nsv531613, nsv531614, nsv529233) are listed (Figure 2A). The clinical information provided for these individuals was limited but indicated developmental delay in 3/4 case subjects and unspecified abnormalities of the central nervous system in the fourth (dbVar: nsv529233). In line with our findings, all four deletions listed in this database were classified as pathogenic. There are further genomic alterations of *NFIB* reported in individuals with

autism spectrum disorder (ASD): a paternally inherited intronic loss of 8,341 bp in intron 2, a sequence variant affecting the 3′ splice region of exon 4, and a balanced cytogenetic abnormality affecting *NFIB*.[73–75]

In addition, genome-wide association studies have implicated single-nucleotide polymorphisms within or near *NFIB* with behavioral phenotypes. For instance, intronic SNP rs4741351 has been associated with decreased learning attainment and rs1322987 with delayed story telling.[76,77] Furthermore, SNPs in *NFIB* have also been associated with bipolar disorder and schizophrenia.[78–81] Interestingly, an ASD-associated intronic SNP in Engrailed 2 removes an NFIB-binding site and results in reduced Engrailed 2 expression,[82] suggesting that this gene is potentially an important downstream target of *NFIB*. Taken together, *NFIB* may be more broadly implicated in ID and behavioral phenotypes than in the cohort presented in this paper.

NFIB Haploinsufficiency Causes a Syndrome with Macrocephaly and Intellectual Disability

We report 18 individuals with ID in which we identified alterations of *NFIB*, including partial and whole gene deletions with a variable number of neighboring genes, as well as seven pathogenic sequence variants. Based on these findings, we propose that haploinsufficiency of *NFIB* is the common underlying pathogenic mechanism, thus introducing *NFIB* mutations as causative for ID. The 18 affected individuals shared a similar phenotype of mild ID, muscular hypotonia, speech delay, attention deficit disorder, and variable behavioral anomalies. Head circumference was above the mean in 16/16, and 13/16 individuals had absolute macrocephaly. Other structural brain anomalies including corpus callosum dysgenesis may be present. Although congenital malformations and facial anomalies that allow clinical recognition of the disease are not part of the presentation, all individuals share some minor dysmorphic features. We propose that *NFIB* haploinsufficiency causes a macrocephaly-intellectual disability syndrome overlapping with *NFIA* and *NFIX* haploinsufficiency phenotypes.

Accession Numbers

The ClinVar accession numbers for the *NFIB* sequence variants and *NFIB* deletions reported in this paper are as follows: c.109C>T (p.Arg37*), SCV000803743.1; c.265C>T (p.Arg89*), SCV000803744.1; c.341A>C (p.Lys114Thr), SCV000803745.1; c.376A>G (p.Lys126Glu), SCV000803746.1; c.395T>C (p.Leu132Pro), SCV000803747.1; c.758_759dupTG (p.Asn254*), SCV000803748.1; c.1063_1076del (p.Ile355Serfs*48), SCV000803749.1; c.1067C>T (p.Ser356Leu), SCV000803750.1; arr[hg19] 9p23p22.3(14098659_14324147)x1, SCV000809030; arr[hg19] 9p23p22.3(14102175_14386038)x1, SCV000809031; arr[hg19] 9p23p22.3(13974415_14286259)x1, SCV000809032; arr[hg19] 9p23p22.3(13106806_14639971)x1, SCV000809033; arr[hg19] 9p23p22.3(13034407_14653394)x1, SCV000809034; arr[hg19] 9p23p22.2(14178768_16619009)x1, SCV000809035; arr[hg19] 9p23p22.2(13563537_18491752)x1, SCV000809036; arr[hg19] 9p23p22.2(13739630_18023839)x1, SCV000809037.

Supplemental Data

Supplemental Data include a Supplemental Note on case reports, four figures, two tables, Supplemental Methods, and Acknowledgments, and can be found with this article online at https://doi.org/10.1016/j.ajhg.2018.10.006.

Acknowledgments

We would like to thank the families for their collaboration and contribution to this project. We thank Prof. William D. Richardson and Dr. Nicoletta Kessaris, Wolfson Institute for Biomedical Research, University College London, for providing the Emx1iCre mice for this project. We would like to thank Dr. Nyoman Kurniawan of the Centre for Advanced Imaging, the University of Queensland, for his technical expertise and assistance in conducting the *ex vivo* mouse brain MRI. In additional, we would also like to thank the members of the IRC[5] consortium for their support.

This work was supported by grants from the National Health and Medical Research Council Australia (GNT1100443 to L.J.R.), the French Ministry of Health (PHRC national 2008/2008-A00515-50), Regional Council of Burgundy/Dijon University hospital (PARI 2012), The Genesis Foundation for Children, the US National Institutes of Health under NINDS grants (1R01NS092772 and 234567890 to W.B.D.; 1R01NS058721 to W.B.D. and E.H.S.; and K08NS092898 to G.M.M.), and Jordan's Guardian Angels (G.M.M.). J.W.C.L. was supported by an International Postgraduate Research Scholarship and UQ Centennial Scholarship. R.M.G. was supported by NYSTEM grants (C026714, C026429, and C030133). R.J.D. was supported by Brain Injured Children's Aftercare Recovery Endeavours (BICARE) Fellowship. L.J.R. was supported by an NHMRC Principal Research Fellowship (GNT1005751). M.Z. was supported by a grant from the German Ministry of Education and Research (BMBF) (GeNeRARe 01GM1519A). We acknowledge the Linkage Infrastructure, Equipment and Facilities (LIEF) grant (LE100100074) awarded to the Queensland Brain Institute for the Slide Scanner and the facilities of the National Imaging Facility (NIF) at the Centre for Advanced Imaging, University of Queensland, used in the animal experiments. The content is solely the responsibility of the authors and does not necessarily represent the official views of the funding sources.

Declaration of Interests

The authors declare no competing interests.

Received: July 4, 2018
Accepted: October 3, 2018
Published: November 1, 2018

Web Resources

1000 Genomes, http://www.internationalgenome.org/
ClinVar, https://www.ncbi.nlm.nih.gov/clinvar/
Database of Genomic Variants (DGV), http://dgv.tcag.ca/dgv/app/home

dbSNP, https://www.ncbi.nlm.nih.gov/projects/SNP/
dbVar, http://www.ncbi.nlm.nih.gov/dbvar/
DECIPHER, https://decipher.sanger.ac.uk/
ECARUCA, http://ecaruca.radboudumc.nl:8080/ecaruca/
Ensembl Genome Browser, http://www.ensembl.org/index.html
ExAC Browser, http://exac.broadinstitute.org/
GenBank, https://www.ncbi.nlm.nih.gov/genbank/
Head circumference calculator, https://simulconsult.com/resources/measurement.html?type=head
MutationTaster, http://www.mutationtaster.org/
NHLBI Exome Sequencing Project (ESP) Exome Variant Server, http://evs.gs.washington.edu/EVS/
OMIM, http://www.omim.org/
PolyPhen-2, http://genetics.bwh.harvard.edu/pph2/
PredictSNP2, https://loschmidt.chemi.muni.cz/predictsnp2/
PROVEAN, http://provean.jcvi.org

References

1. Campbell, C.E., Piper, M., Plachez, C., Yeh, Y.T., Baizer, J.S., Osinski, J.M., Litwack, E.D., Richards, L.J., and Gronostajski, R.M. (2008). The transcription factor Nfix is essential for normal brain development. BMC Dev. Biol. *8*, 52.
2. das Neves, L., Duchala, C.S., Tolentino-Silva, F., Haxhiu, M.A., Colmenares, C., Macklin, W.B., Campbell, C.E., Butz, K.G., and Gronostajski, R.M. (1999). Disruption of the murine nuclear factor I-A gene (Nfia) results in perinatal lethality, hydrocephalus, and agenesis of the corpus callosum. Proc. Natl. Acad. Sci. USA *96*, 11946–11951.
3. Gronostajski, R.M. (2000). Roles of the NFI/CTF gene family in transcription and development. Gene *249*, 31–45.
4. Mason, S., Piper, M., Gronostajski, R.M., and Richards, L.J. (2009). Nuclear factor one transcription factors in CNS development. Mol. Neurobiol. *39*, 10–23.
5. Piper, M., Moldrich, R.X., Lindwall, C., Little, E., Barry, G., Mason, S., Sunn, N., Kurniawan, N.D., Gronostajski, R.M., and Richards, L.J. (2009). Multiple non-cell-autonomous defects underlie neocortical callosal dysgenesis in Nfib-deficient mice. Neural Dev. *4*, 43.
6. Shu, T., Butz, K.G., Plachez, C., Gronostajski, R.M., and Richards, L.J. (2003). Abnormal development of forebrain midline glia and commissural projections in Nfia knock-out mice. J. Neurosci. *23*, 203–212.
7. Steele-Perkins, G., Plachez, C., Butz, K.G., Yang, G., Bachurski, C.J., Kinsman, S.L., Litwack, E.D., Richards, L.J., and Gronostajski, R.M. (2005). The transcription factor gene Nfib is essential for both lung maturation and brain development. Mol. Cell. Biol. *25*, 685–698.
8. Betancourt, J., Katzman, S., and Chen, B. (2014). Nuclear factor one B regulates neural stem cell differentiation and axonal projection of corticofugal neurons. J. Comp. Neurol. *522*, 6–35.
9. Gobius, I., Morcom, L., Suárez, R., Bunt, J., Bukshpun, P., Reardon, W., Dobyns, W.B., Rubenstein, J.L., Barkovich, A.J., Sherr, E.H., and Richards, L.J. (2016). Astroglial-mediated remodeling of the interhemispheric midline is required for the formation of the corpus callosum. Cell Rep. *17*, 735–747.
10. Chen, C.P., Su, Y.N., Chen, Y.Y., Chern, S.R., Liu, Y.P., Wu, P.C., Lee, C.C., Chen, Y.T., and Wang, W. (2011). Chromosome 1p32-p31 deletion syndrome: prenatal diagnosis by array comparative genomic hybridization using uncultured amniocytes and association with NFIA haploinsufficiency, ventriculomegaly, corpus callosum hypogenesis, abnormal external genitalia, and intrauterine growth restriction. Taiwan. J. Obstet. Gynecol. *50*, 345–352.
11. Ji, J., Salamon, N., and Quintero-Rivera, F. (2014). Microdeletion of 1p32-p31 involving NFIA in a patient with hypoplastic corpus callosum, ventriculomegaly, seizures and urinary tract defects. Eur. J. Med. Genet. *57*, 267–268.
12. Koehler, U., Holinski-Feder, E., Ertl-Wagner, B., Kunz, J., von Moers, A., von Voss, H., and Schell-Apacik, C. (2010). A novel 1p31.3p32.2 deletion involving the NFIA gene detected by array CGH in a patient with macrocephaly and hypoplasia of the corpus callosum. Eur. J. Pediatr. *169*, 463–468.
13. Lu, W., Quintero-Rivera, F., Fan, Y., Alkuraya, F.S., Donovan, D.J., Xi, Q., Turbe-Doan, A., Li, Q.G., Campbell, C.G., Shanske, A.L., et al. (2007). NFIA haploinsufficiency is associated with a CNS malformation syndrome and urinary tract defects. PLoS Genet. *3*, e80.
14. Negishi, Y., Miya, F., Hattori, A., Mizuno, K., Hori, I., Ando, N., Okamoto, N., Kato, M., Tsunoda, T., Yamasaki, M., et al. (2015). Truncating mutation in NFIA causes brain malformation and urinary tract defects. Hum Genome Var *2*, 15007.
15. Nyboe, D., Kreiborg, S., Kirchhoff, M., and Hove, H.B. (2015). Familial craniosynostosis associated with a microdeletion involving the NFIA gene. Clin. Dysmorphol. *24*, 109–112.
16. Rao, A., O'Donnell, S., Bain, N., Meldrum, C., Shorter, D., and Goel, H. (2014). An intragenic deletion of the NFIA gene in a patient with a hypoplastic corpus callosum, craniofacial abnormalities and urinary tract defects. Eur. J. Med. Genet. *57*, 65–70.
17. Zhao, W.W. (2013). Intragenic deletion of RBFOX1 associated with neurodevelopmental/neuropsychiatric disorders and possibly other clinical presentations. Mol. Cytogenet. *6*, 26.
18. Mikhail, F.M., Lose, E.J., Robin, N.H., Descartes, M.D., Rutledge, K.D., Rutledge, S.L., Korf, B.R., and Carroll, A.J. (2011). Clinically relevant single gene or intragenic deletions encompassing critical neurodevelopmental genes in patients with developmental delay, mental retardation, and/or autism spectrum disorders. Am. J. Med. Genet. A. *155A*, 2386–2396.
19. Revah-Politi, A., Ganapathi, M., Bier, L., Cho, M.T., Goldstein, D.B., Hemati, P., Iglesias, A., Juusola, J., Pappas, J., Petrovski, S., et al. (2017). Loss-of-function variants in NFIA provide further support that NFIA is a critical gene in 1p32-p31 deletion syndrome: A four patient series. Am. J. Med. Genet. A. *173*, 3158–3164.
20. Dong, H.Y., Zeng, H., Hu, Y.Q., Xie, L., Wang, J., Wang, X.Y., Yang, Y.F., and Tan, Z.P. (2016). 19p13.2 Microdeletion including NFIX associated with overgrowth and intellectual disability suggestive of Malan syndrome. Mol. Cytogenet. *9*, 71.
21. Gurrieri, F., Cavaliere, M.L., Wischmeijer, A., Mammì, C., Neri, G., Pisanti, M.A., Rodella, G., Laganà, C., and Priolo, M. (2015). NFIX mutations affecting the DNA-binding domain cause a peculiar overgrowth syndrome (Malan syndrome): a new patients series. Eur. J. Med. Genet. *58*, 488–491.
22. Jezela-Stanek, A., Kucharczyk, M., Falana, K., Jurkiewicz, D., Mlynek, M., Wicher, D., Rydzanicz, M., Kugaudo, M., Cieslikowska, A., Ciara, E., et al. (2016). Malan syndrome (Sotos syndrome 2) in two patients with 19p13.2 deletion encompassing NFIX gene and novel NFIX sequence variant. Biomed. Pap. Med. Fac. Univ. Palacky Olomouc Czech Repub. *160*, 161–167.

23. Klaassens, M., Morrogh, D., Rosser, E.M., Jaffer, F., Vreeburg, M., Bok, L.A., Segboer, T., van Belzen, M., Quinlivan, R.M., Kumar, A., et al. (2015). Malan syndrome: Sotos-like overgrowth with de novo NFIX sequence variants and deletions in six new patients and a review of the literature. Eur. J. Hum. Genet. *23*, 610–615.
24. Malan, V., Rajan, D., Thomas, S., Shaw, A.C., Louis Dit Picard, H., Layet, V., Till, M., van Haeringen, A., Mortier, G., Nampoothiri, S., et al. (2010). Distinct effects of allelic NFIX mutations on nonsense-mediated mRNA decay engender either a Sotos-like or a Marshall-Smith syndrome. Am. J. Hum. Genet. *87*, 189–198.
25. Oshima, T., Hara, H., Takeda, N., Hasumi, E., Kuroda, Y., Taniguchi, G., Inuzuka, R., Nawata, K., Morita, H., and Komuro, I. (2017). A novel mutation of *NFIX* causes Sotos-like syndrome (Malan syndrome) complicated with thoracic aortic aneurysm and dissection. Hum Genome Var *4*, 17022.
26. Shimojima, K., Okamoto, N., Tamasaki, A., Sangu, N., Shimada, S., and Yamamoto, T. (2015). An association of 19p13.2 microdeletions with Malan syndrome and Chiari malformation. Am. J. Med. Genet. A. *167A*, 724–730.
27. Aggarwal, A., Nguyen, J., Rivera-Davila, M., and Rodriguez-Buritica, D. (2017). Marshall-Smith syndrome: Novel pathogenic variant and previously unreported associations with precocious puberty and aortic root dilatation. Eur. J. Med. Genet. *60*, 391–394.
28. Martinez, F., Marín-Reina, P., Sanchis-Calvo, A., Perez-Aytés, A., Oltra, S., Roselló, M., Mayo, S., Monfort, S., Pantoja, J., and Orellana, C. (2015). Novel mutations of NFIX gene causing Marshall-Smith syndrome or Sotos-like syndrome: one gene, two phenotypes. Pediatr. Res. *78*, 533–539.
29. Schanze, D., Neubauer, D., Cormier-Daire, V., Delrue, M.A., Dieux-Coeslier, A., Hasegawa, T., Holmberg, E.E., Koenig, R., Krueger, G., Schanze, I., et al. (2014). Deletions in the 3′ part of the NFIX gene including a recurrent Alu-mediated deletion of exon 6 and 7 account for previously unexplained cases of Marshall-Smith syndrome. Hum. Mutat. *35*, 1092–1100.
30. Chaudhry, A.Z., Lyons, G.E., and Gronostajski, R.M. (1997). Expression patterns of the four nuclear factor I genes during mouse embryogenesis indicate a potential role in development. Dev. Dyn. *208*, 313–325.
31. Bunt, J., Lim, J.W., Zhao, L., Mason, S., and Richards, L.J. (2015). PAX6 does not regulate Nfia and Nfib expression during neocortical development. Sci. Rep. *5*, 10668.
32. Plachez, C., Lindwall, C., Sunn, N., Piper, M., Moldrich, R.X., Campbell, C.E., Osinski, J.M., Gronostajski, R.M., and Richards, L.J. (2008). Nuclear factor I gene expression in the developing forebrain. J. Comp. Neurol. *508*, 385–401.
33. Driller, K., Pagenstecher, A., Uhl, M., Omran, H., Berlis, A., Gründer, A., and Sippel, A.E. (2007). Nuclear factor I X deficiency causes brain malformation and severe skeletal defects. Mol. Cell. Biol. *27*, 3855–3867.
34. Bunt, J., Osinki, J., Lim, J.W.C., Vidovic, D., Ye, Y., Zalucki, O., O'Connor, T., Harris, L., Gronostajski, R., Richards, L.J., et al. (2017). Combined allelic dosage of Nfia and Nfib regulates cortical development. BNA. Published online November 22, 2017. https://doi.org/10.1177/2398212817739433.
35. Sajan, S.A., Fernandez, L., Nieh, S.E., Rider, E., Bukshpun, P., Wakahiro, M., Christian, S.L., Rivière, J.B., Sullivan, C.T., Sudi, J., et al. (2013). Both rare and de novo copy number variants are prevalent in agenesis of the corpus callosum but not in cerebellar hypoplasia or polymicrogyria. PLoS Genet. *9*, e1003823.
36. Sobreira, N., Schiettecatte, F., Valle, D., and Hamosh, A. (2015). GeneMatcher: a matching tool for connecting investigators with an interest in the same gene. Hum. Mutat. *36*, 928–930.
37. Zhang, X., Snijders, A., Segraves, R., Zhang, X., Niebuhr, A., Albertson, D., Yang, H., Gray, J., Niebuhr, E., Bolund, L., and Pinkel, D. (2005). High-resolution mapping of genotype-phenotype relationships in cri du chat syndrome using array comparative genomic hybridization. Am. J. Hum. Genet. *76*, 312–326.
38. MacDonald, J.R., Ziman, R., Yuen, R.K., Feuk, L., and Scherer, S.W. (2014). The Database of Genomic Variants: a curated collection of structural variation in the human genome. Nucleic Acids Res. *42*, D986–D992.
39. Firth, H.V., Richards, S.M., Bevan, A.P., Clayton, S., Corpas, M., Rajan, D., Van Vooren, S., Moreau, Y., Pettett, R.M., and Carter, N.P. (2009). DECIPHER: Database of Chromosomal Imbalance and Phenotype in Humans Using Ensembl Resources. Am. J. Hum. Genet. *84*, 524–533.
40. Vulto-van Silfhout, A.T., van Ravenswaaij, C.M., Hehir-Kwa, J.Y., Verwiel, E.T., Dirks, R., van Vooren, S., Schinzel, A., de Vries, B.B., and de Leeuw, N. (2013). An update on ECARUCA, the European Cytogeneticists Association Register of Unbalanced Chromosome Aberrations. Eur. J. Med. Genet. *56*, 471–474.
41. Landrum, M.J., Lee, J.M., Benson, M., Brown, G., Chao, C., Chitipiralla, S., Gu, B., Hart, J., Hoffman, D., Hoover, J., et al. (2016). ClinVar: public archive of interpretations of clinically relevant variants. Nucleic Acids Res. *44* (D1), D862–D868.
42. Bendl, J., Musil, M., Štourač, J., Zendulka, J., Damborský, J., and Brezovský, J. (2016). PredictSNP2: a unified platform for accurately evaluating SNP effects by exploiting the different characteristics of variants in distinct genomic regions. PLoS Comput. Biol. *12*, e1004962.
43. Schwarz, J.M., Cooper, D.N., Schuelke, M., and Seelow, D. (2014). MutationTaster2: mutation prediction for the deep-sequencing age. Nat. Methods *11*, 361–362.
44. Kumar, P., Henikoff, S., and Ng, P.C. (2009). Predicting the effects of coding non-synonymous variants on protein function using the SIFT algorithm. Nat. Protoc. *4*, 1073–1081.
45. Adzhubei, I.A., Schmidt, S., Peshkin, L., Ramensky, V.E., Gerasimova, A., Bork, P., Kondrashov, A.S., and Sunyaev, S.R. (2010). A method and server for predicting damaging missense mutations. Nat. Methods *7*, 248–249.
46. Piper, M., Barry, G., Harvey, T.J., McLeay, R., Smith, A.G., Harris, L., Mason, S., Stringer, B.W., Day, B.W., Wray, N.R., et al. (2014). NFIB-mediated repression of the epigenetic factor Ezh2 regulates cortical development. J. Neurosci. *34*, 2921–2930.
47. Olmsted, J.B., Carlson, K., Klebe, R., Ruddle, F., and Rosenbaum, J. (1970). Isolation of microtubule protein from cultured mouse neuroblastoma cells. Proc. Natl. Acad. Sci. USA *65*, 129–136.
48. Westermark, B. (1973). The deficient density-dependent growth control of human malignant glioma cells and virus-transformed glia-like cells in culture. Int. J. Cancer *12*, 438–451.
49. Zhou, B.Y., Liu, Y., Kim, Bo., Xiao, Y., and He, J.J. (2004). Astrocyte activation and dysfunction and neuron death by HIV-1 Tat expression in astrocytes. Mol. Cell. Neurosci. *27*, 296–305.
50. Chang, C.Y., Pasolli, H.A., Giannopoulou, E.G., Guasch, G., Gronostajski, R.M., Elemento, O., and Fuchs, E. (2013). NFIB

is a governor of epithelial-melanocyte stem cell behaviour in a shared niche. Nature *495*, 98–102.

51. Hsu, Y.C., Osinski, J., Campbell, C.E., Litwack, E.D., Wang, D., Liu, S., Bachurski, C.J., and Gronostajski, R.M. (2011). Mesenchymal nuclear factor I B regulates cell proliferation and epithelial differentiation during lung maturation. Dev. Biol. *354*, 242–252.
52. Kessaris, N., Fogarty, M., Iannarelli, P., Grist, M., Wegner, M., and Richardson, W.D. (2006). Competing waves of oligodendrocytes in the forebrain and postnatal elimination of an embryonic lineage. Nat. Neurosci. *9*, 173–179.
53. Piper, M., Harris, L., Barry, G., Heng, Y.H., Plachez, C., Gronostajski, R.M., and Richards, L.J. (2011). Nuclear factor one X regulates the development of multiple cellular populations in the postnatal cerebellum. J. Comp. Neurol. *519*, 3532–3548.
54. Lim, J.W., Donahoo, A.L., Bunt, J., Edwards, T.J., Fenlon, L.R., Liu, Y., Zhou, J., Moldrich, R.X., Piper, M., Gobius, I., et al. (2015). EMX1 regulates NRP1-mediated wiring of the mouse anterior cingulate cortex. Development *142*, 3746–3757.
55. Moldrich, R.X., Pannek, K., Hoch, R., Rubenstein, J.L., Kurniawan, N.D., and Richards, L.J. (2010). Comparative mouse brain tractography of diffusion magnetic resonance imaging. Neuroimage *51*, 1027–1036.
56. Ma, Y., Hof, P.R., Grant, S.C., Blackband, S.J., Bennett, R., Slatest, L., McGuigan, M.D., and Benveniste, H. (2005). A three-dimensional digital atlas database of the adult C57BL/6J mouse brain by magnetic resonance microscopy. Neuroscience *135*, 1203–1215.
57. Alby, C., Malan, V., Boutaud, L., Marangoni, M.A., Bessières, B., Bonniere, M., Ichkou, A., Elkhartoufi, N., Bahi-Buisson, N., Sonigo, P., et al. (2016). Clinical, genetic and neuropathological findings in a series of 138 fetuses with a corpus callosum malformation. Birth Defects Res. A Clin. Mol. Teratol. *106*, 36–46.
58. Liu, Y., Bernard, H.U., and Apt, D. (1997). NFI-B3, a novel transcriptional repressor of the nuclear factor I family, is generated by alternative RNA processing. J. Biol. Chem. *272*, 10739–10745.
59. Stringer, B.W., Bunt, J., Day, B.W., Barry, G., Jamieson, P.R., Ensbey, K.S., Bruce, Z.C., Goasdoué, K., Vidal, H., Charmsaz, S., et al. (2016). Nuclear factor one B (NFIB) encodes a subtype-specific tumour suppressor in glioblastoma. Oncotarget *7*, 29306–29320.
60. Brun, M., Coles, J.E., Monckton, E.A., Glubrecht, D.D., Bisgrove, D., and Godbout, R. (2009). Nuclear factor I regulates brain fatty acid-binding protein and glial fibrillary acidic protein gene expression in malignant glioma cell lines. J. Mol. Biol. *391*, 282–300.
61. Barry, G., Piper, M., Lindwall, C., Moldrich, R., Mason, S., Little, E., Sarkar, A., Tole, S., Gronostajski, R.M., and Richards, L.J. (2008). Specific glial populations regulate hippocampal morphogenesis. J. Neurosci. *28*, 12328–12340.
62. Huang, N., Lee, I., Marcotte, E.M., and Hurles, M.E. (2010). Characterising and predicting haploinsufficiency in the human genome. PLoS Genet. *6*, e1001154.
63. Lek, M., Karczewski, K.J., Minikel, E.V., Samocha, K.E., Banks, E., Fennell, T., O'Donnell-Luria, A.H., Ware, J.S., Hill, A.J., Cummings, B.B., et al.; Exome Aggregation Consortium (2016). Analysis of protein-coding genetic variation in 60,706 humans. Nature *536*, 285–291.
64. Gründer, A., Ebel, T.T., Mallo, M., Schwarzkopf, G., Shimizu, T., Sippel, A.E., and Schrewe, H. (2002). Nuclear factor I-B (Nfib) deficient mice have severe lung hypoplasia. Mech. Dev. *112*, 69–77.
65. Gobius, I., Suárez, R., Morcom, L., Paolino, A., Edwards, T.J., Kozulin, P., and Richards, L.J. (2017). Astroglial-mediated remodeling of the interhemispheric midline during telencephalic development is exclusive to eutherian mammals. Neural Dev. *12*, 9.
66. Chen, K.S., Harris, L., Lim, J.W.C., Harvey, T.J., Piper, M., Gronostajski, R.M., Richards, L.J., and Bunt, J. (2017). Differential neuronal and glial expression of nuclear factor I proteins in the cerebral cortex of adult mice. J. Comp. Neurol. *525*, 2465–2483.
67. Harris, L., Zalucki, O., Gobius, I., McDonald, H., Osinki, J., Harvey, T.J., Essebier, A., Vidovic, D., Gladwyn-Ng, I., Burne, T.H., et al. (2016). Transcriptional regulation of intermediate progenitor cell generation during hippocampal development. Development *143*, 4620–4630.
68. Priolo, M., Schanze, D., Tatton-Brown, K., Mulder, P.A., Tenorio, J., Kooblall, K., Acero, I.H., Alkuraya, F.S., Arias, P., Bernardini, L., et al. (2018). Further delineation of Malan syndrome. Hum. Mutat. *39*, 1226–1237.
69. Yoneda, Y., Saitsu, H., Touyama, M., Makita, Y., Miyamoto, A., Hamada, K., Kurotaki, N., Tomita, H., Nishiyama, K., Tsurusaki, Y., et al. (2012). Missense mutations in the DNA-binding/dimerization domain of NFIX cause Sotos-like features. J. Hum. Genet. *57*, 207–211.
70. Tatton-Brown, K., Loveday, C., Yost, S., Clarke, M., Ramsay, E., Zachariou, A., Elliott, A., Wylie, H., Ardissone, A., Rittinger, O., et al.; Childhood Overgrowth Collaboration (2017). Mutations in epigenetic regulation genes are a major cause of overgrowth with intellectual disability. Am. J. Hum. Genet. *100*, 725–736.
71. Farwell, K.D., Shahmirzadi, L., El-Khechen, D., Powis, Z., Chao, E.C., Tippin Davis, B., Baxter, R.M., Zeng, W., Mroske, C., Parra, M.C., et al. (2015). Enhanced utility of family-centered diagnostic exome sequencing with inheritance model-based analysis: results from 500 unselected families with undiagnosed genetic conditions. Genet. Med. *17*, 578–586.
72. Landrum, M.J., Lee, J.M., Riley, G.R., Jang, W., Rubinstein, W.S., Church, D.M., and Maglott, D.R. (2014). ClinVar: public archive of relationships among sequence variation and human phenotype. Nucleic Acids Res. *42*, D980–D985.
73. Prasad, A., Merico, D., Thiruvahindrapuram, B., Wei, J., Lionel, A.C., Sato, D., Rickaby, J., Lu, C., Szatmari, P., Roberts, W., et al. (2012). A discovery resource of rare copy number variations in individuals with autism spectrum disorder. G3 (Bethesda) *2*, 1665–1685.
74. Iossifov, I., Ronemus, M., Levy, D., Wang, Z., Hakker, I., Rosenbaum, J., Yamrom, B., Lee, Y.H., Narzisi, G., Leotta, A., et al. (2012). De novo gene disruptions in children on the autistic spectrum. Neuron *74*, 285–299.
75. Redin, C., Brand, H., Collins, R.L., Kammin, T., Mitchell, E., Hodge, J.C., Hanscom, C., Pillalamarri, V., Seabra, C.M., Abbott, M.A., et al. (2017). The genomic landscape of balanced cytogenetic abnormalities associated with human congenital anomalies. Nat. Genet. *49*, 36–45.
76. Okbay, A., Beauchamp, J.P., Fontana, M.A., Lee, J.J., Pers, T.H., Rietveld, C.A., Turley, P., Chen, G.B., Emilsson, V., Meddens, S.F., et al.; LifeLines Cohort Study (2016). Genome-wide

association study identifies 74 loci associated with educational attainment. Nature *533*, 539–542.

77. Cirulli, E.T., Kasperaviciūte, D., Attix, D.K., Need, A.C., Ge, D., Gibson, G., and Goldstein, D.B. (2010). Common genetic variation and performance on standardized cognitive tests. Eur. J. Hum. Genet. *18*, 815–820.
78. Le-Niculescu, H., Patel, S.D., Bhat, M., Kuczenski, R., Faraone, S.V., Tsuang, M.T., McMahon, F.J., Schork, N.J., Nurnberger, J.I., Jr., and Niculescu, A.B., 3rd. (2009). Convergent functional genomics of genome-wide association data for bipolar disorder: comprehensive identification of candidate genes, pathways and mechanisms. Am. J. Med. Genet. B. Neuropsychiatr. Genet. *150B*, 155–181.
79. Willour, V.L., Seifuddin, F., Mahon, P.B., Jancic, D., Pirooznia, M., Steele, J., Schweizer, B., Goes, F.S., Mondimore, F.M., Mackinnon, D.F., et al.; Bipolar Genome Study Consortium (2012). A genome-wide association study of attempted suicide. Mol. Psychiatry *17*, 433–444.
80. Segurado, R., Detera-Wadleigh, S.D., Levinson, D.F., Lewis, C.M., Gill, M., Nurnberger, J.I., Jr., Craddock, N., DePaulo, J.R., Baron, M., Gershon, E.S., et al. (2003). Genome scan meta-analysis of schizophrenia and bipolar disorder, part III: Bipolar disorder. Am. J. Hum. Genet. *73*, 49–62.
81. Gupta, C.N., Chen, J., Liu, J., Damaraju, E., Wright, C., Perrone-Bizzozero, N.I., Pearlson, G., Luo, L., Michael, A.M., Turner, J.A., and Calhoun, V.D. (2015). Genetic markers of white matter integrity in schizophrenia revealed by parallel ICA. Front. Hum. Neurosci. *9*, 100.
82. Choi, J., Ababon, M.R., Matteson, P.G., and Millonig, J.H. (2012). Cut-like homeobox 1 and nuclear factor I/B mediate ENGRAILED2 autism spectrum disorder-associated haplotype function. Hum. Mol. Genet. *21*, 1566–1580.

The American Journal of Human Genetics, Volume *103*

Supplemental Data

NFIB Haploinsufficiency Is Associated with Intellectual Disability and Macrocephaly

Ina Schanze, Jens Bunt, Jonathan W.C. Lim, Denny Schanze, Ryan J. Dean, Marielle Alders, Patricia Blanchet, Tania Attié-Bitach, Siren Berland, Steven Boogert, Sangamitra Boppudi, Caitlin J. Bridges, Megan T. Cho, William B. Dobyns, Dian Donnai, Jessica Douglas, Dawn L. Earl, Timothy J. Edwards, Laurence Faivre, Brieana Fregeau, David Genevieve, Marion Gérard, Vincent Gatinois, Muriel Holder-Espinasse, Samuel F. Huth, Kosuke Izumi, Bronwyn Kerr, Elodie Lacaze, Phillis Lakeman, Sonal Mahida, Ghayda M. Mirzaa, Sian M. Morgan, Catherine Nowak, Hilde Peeters, Florence Petit, Daniela T. Pilz, Jacques Puechberty, Eyal Reinstein, Jean-Baptiste Rivière, Avni B. Santani, Anouck Schneider, Elliott H. Sherr, Constance Smith-Hicks, Ilse Wieland, Elaine Zackai, Xiaonan Zhao, Richard M. Gronostajski, Martin Zenker, and Linda J. Richards

SUPPLEMENTAL DATA

Supplemental Note: Case Reports.

Proband 1 *p.(Arg37*)*

This 16-year old male proband is the oldest child from a family of three. He has a healthy brother and sister. His sister had a surgical correction of a ventricular septum defect.

The proband was born after an uncomplicated pregnancy at a gestational age of 41 weeks by vacuum extraction with a low birth weight of 2750 g. There was a motor and speech developmental delay, which was assigned to agenesis of the corpus callosum, resulting in an intellectual deficit (verbal IQ is 60; non-verbal IQ is 80). Other health complaints were: obstipation (in early childhood), bilateral hernia inguinalis at young age (between first and second year of his life). He suffered from frequent recurring ear infections due to an anatomically abnormal Eustachian tube, resulting in some hearing loss for which no hearing aids are needed. He has difficulties in falling asleep. Facial dysmorphic features of this proband are: he has a relatively large head circumference of 60.5 cm (+3.76 SD) with a height of 173 cm (+0.2 SD) and a weight of 56 kg (-0.42 SD). He has a large forehead with a high frontal hairline, with a frontal tuft, down slanting palpebral fissures, a high nasal bridge, a small columella, small ears, a relatively large mouth with a high palate, some small fissures in the tongue, and a large pointing chin. There is a pectus excavatum with widely spaced nipples. There is no abdominal wall defect but the navel shows laxity. The hands are small. The feet are large; there is bilateral pes planus, a sandal gap and broad halluces. There is no hypo- or hyperpigmentations, apart from 10 to 20 simple naevi on the back and one capillary malformation (“haemangioma”) on the back side of the upper left arm.

Proband 2 *p.(Arg89*)*

This 7-year old male proband is the youngest of two children from a non-consanguineous family. He has a healthy sister, as well as two healthy maternal half-sisters. The proband was born following an uncomplicated pregnancy. However, his mother has a history of drug use. He was born full term with a birth weight of 3997 g. At age 6 months, his OFC was noted to be above the 95th percentile. He was subsequently noted to have developmental delays. He first walked at about 1 year of age, but his language development was more delayed; his first words were between 1.5 and 2 years. His speech is limited to single words and short phrases. He was enrolled in speech therapy in early childhood. The proband also has several behavioral problems including anger control problems suggesting possible oppositional-defiant behavior. His attention span is described as being short. He has a history of episodic tachycardia and underwent a cardiology evaluation that included an electrocardiogram which was normal, with no further intervention. On last assessment at age 6 years and 8 months, his height was 124.9 cm (+0.58 SD), weight 23 kg (-0.02 SD) and occipito-frontal circumference was 57.2 cm (+3.94 SD). Examination revealed macrocephaly with dolichocephaly, broad and prominent forehead, bifid tip of the uvula, mildly flat mid-face, flat nose, and fullness of the nasolabial folds. Thumbs and great toes were mildly broad, with a mild sandal-gap toe deformity. Skin examination revealed two hyperpigmented macules and several nevi over the trunk and extremities. Brain MRI at age 1 year and 9 months showed macrocephaly with a prominent forehead, mildly in folded gyri in the perisylvian regions but otherwise normal gyral pattern, increased perivascular spaces in the caudal basal ganglia, diffusely thin white matter, and a thin corpus callosum. He also had mild cerebellar tonsillar ectopia, but no Chiari malformation.

Proband 3 *p.(Lys114Thr)*

This proband was almost 7 years old when he presented to the neurogenetics clinic and was at that time diagnosed with ASD, Attention Deficit Hyperactive Disorder, Global Developmental Delay affecting language, cognition, fine and gross motor skills. He was the product of a twin pregnancy that was conceived via in−vitro fertilization and was otherwise uncomplicated. He was born to non−consanguineous parents; a 36-year-old mother and 30-year-old father. His birth weight was 2499 g and he was born via emergency C-section secondary to late decelerations. He had multiple otitis media and required pressure equalizing tubes. He was diagnosed with obstructive sleep apnea at 1 year old and esotropia of the right eye both resolved with intervention. He walked at 18 months old, used a mature pincer grasp after 1 year old and started using words around 4.5 years old.

His twin sister shows unremarkable development. Maternal history is significant for migraines and vasovagal syncope and there is a paternal history of learning disabilities. Extended family history is notable for hypertension, anxiety, diabetes mellitus, anxiety, depression, prostate and breast cancer, thyroid disease, delayed language, learning disabilities and ASD. His clinical exam revealed weight 43.6 kg (+4.17 SD), height 137.0 cm (+2.80 SD) and OFC 58 cm (+5.17 SD). He has wide spaced teeth, flat nasal bridge and small almond shaped eyes. A MRI of the brain is normal. Fragile X DNA testing and SNP microarray were normal. Whole exome sequencing also revealed a variant of uncertain significance c.950A>G (p.Q317R), in the SHANK3 gene (NM_033517.1). Inheritance unknown as his father was unavailable.

Proband 4 *p.(Lys126Glu)*

This male proband was the second of two children of a non-consanguineous, healthy Caucasian couple with unremarkable family history. At conception, the mother was aged 27 and the father was 35 years old. He was born at 39 weeks' gestation after an uneventful pregnancy with a length of 50 cm (-0.06 SD), a weight of 3080 g (+0.77 SD), and an OFC of 39.5 cm (+2.2 SD). He presented with neonatal hypotonia and right cryptorchidism. Developmental milestones were delayed. He started to walk at 2 years old. Speech was delayed with first words around 3 years old. He needed specialized education from the age of 6 onwards.

Currently aged 32, he has mild to moderate intellectual disability and lives in a social care institution. He is able to communicate with short sentences and perform manual tasks. Reading, writing and calculation skills have not been acquired. He is friendly and sociable but suffers from anxiety when faced with change.

On clinical examination, his height was 192.5 cm (+2.25 SD), weight 65 kg -0.49 SD) and OFC 63 cm (+5.52 SD). He has a marfanoid habitus with arachnodactyly, scoliosis, pes planus and sandal gap toes. There is elbow laxity and mild contractures of the fingers flexors. Facial dysmorphism includes brachycephaly, hypertelorism and down-slanting palpebral fissures. Skin examination shows multiple naevi and atrophic scars. He needs optical correction because of nystagmus, strabismus, and astigmatism. ECHO is normal. A cerebro-medullar CT-scan was performed in infancy showing moderate diffuse cerebral atrophy, a cyst of septum pellucidum, and a dorsal meningocele. Because of his intellectual disability and marfanoid habitus, karyotype, array-CGH 44K, testing of *FMR1*, *FBN1*, *FBN2*, *TGBR1* and *TGFBR2* genes were performed and showed normal results.

Proband 5 *p.(Leu132Pro)*

The proband is an 8-year-old male who is the second child of his nonconsanguineous parents. He was born at 40 weeks gestational age to his then 38-year-old mother after an uneventful pregnancy. His birth measurements were normal but frontal bossing was noted. His gross motor development was on time but his speech and fine motor skills were delayed. He has macrocephaly with a prominent occiput (+2.17 SD). Head shape is somewhat dolichocephalic and there is mild frontal bossing at the upper forehead. The paternal head circumference is 59 cm (greater than the 98th percentile). Ears are mildly cupped. He has malar flatness, arched eyebrows with synophrys, a mildly smoothed philtrum, a thin upper vermilion border, and a bifid uvula. He has a translucent skin, thin extremities, and a mildly low muscle tone. Currently, at the age of 8, he has been diagnosed with borderline ID, ASD with sensory integration disorder, aggressive and obsessive behaviors, developmental coordination disorder and attention deficit hyperactivity disorder (ADHD)-combined type. His brain MRI revealed a small rostrum of the corpus callosum. He has sudden unexplained headaches that clear easily with acetaminophen. The proband has undergone chromosomal microarray, *PTEN* sequencing, fragile X testing, sequencing of *TGFBR1* and *TGFBR2*, sequencing of *NSD1*, testing for carbohydrate deficient glycoprotein syndrome, glutaric acid study, and biochemical testing for MPS, all of which were normal.

Probands 6a and 6b *p.(Asn254*)*

Proband 6a is a 33-year-old Jewish female of Sephardi/Ashkenazi origin, the first child of healthy non-consanguineous parents. She was born at term at 2960 g for weight. She had normal tonus and no feeding difficulties, and gross motor development was normal. Yet, fine motor skills and language were delayed. She was evaluated several times and found to have mild developmental delay. There were neither sleeping problems nor seizures; vision and hearing are intact, except for strabismus. She has a normal neurological exam, and normal EEG. She did not have CT or MRI of the brain. She completed 12 years in small classes in the public education system, and is currently working in the public education system as an aid to a girl with special needs. She did not have hospital admissions and her general health is good. At age 26 she gave birth to a male with the same medical condition (P6b). She currently lives at her parents' home with her son and is rather independent. Focused physical examination revealed an overweight female with mild facial dysmorphism including small, hypoteloric eyes, and strabismus. Her son was born at term, via C-section at weight 3900 g. After birth a low muscle tonus with joint laxity were observed and motor milestones were mildly delayed. He has significant language delay and studies in small class at the public-school system. Gross neurological examination as well as vision and hearing were normal. He has similar facial features to his mother.

Proband 7 *p.(Ile355Serfs*48)*

The proband is a 3-year-old girl with developmental delay, hypotonia and ventriculomegaly. Prenatally, she was diagnosed with ventriculomegaly. The ventricles were noted to be enlarged at around 30 weeks of gestation by the prenatal ultrasound. Because of ventriculomegaly, she was born by C-section at 38 weeks of gestation. Her birth weight was 3020 g (-0.77 SD) and length was 48 cm (-0.81 SD). Head circumference at birth was 37cm +1.22 SD). Ventriculomegaly was confirmed postnatally by brain MRI, although surgical intervention was not recommended. In addition, delayed myelination for age was noted. She has experienced several episodes of ear infections, and head CT demonstrated bilateral cholesteatomas. She underwent bilateral tympanomastoidectomy, ear tube placement and adenoidectomy surgeries. She has been diagnosed with bilateral conductive hearing loss. She also has had hypermetropia/hyperopia since 12 months old.

Her development has been mildly delayed. She smiled responsively and laughed at 3 months. She started sitting independently at 8 months and walking independently at 19 months. Her speech and language development has also been delayed. Her first words were at 12 months. At 28 months, she had about 50 words but continued to have poor enunciation and mostly syllables that are interpreted by the context. No developmental regression was noted. The most recent MRI brain at 20 months revealed two small nodules of gray matter heterotopia along the frontal horns of the lateral ventricles. In addition, there were subtle irregularity and thickening along the posterior perisylvian cortex, right greater than left, which raises the possibility of polymicrogyria. Stable prominence of the lateral and third ventricles was demonstrated. No seizures have been observed. Chromosome SNP microarray was unremarkable. Family history is non-contributory.

She was referred to the genetics clinic at 33 months of age. Her height was +0.28 SD, weight was +0.20 SD, and head circumference was +4.72 SD. Her physical examination revealed macrocephaly, broad forehead, frontal bossing, midface hypoplasia, and thin upper lip. She was also noted to have low muscle tone.

Probands 8a and 8b *225kb Del*

The two sisters of 6 and 8 years are in foster care. Their biological mother has learning difficulties, but was not tested genetically. The elder sister (8b) had a cardiac murmur ascribed to mild supravalvular pulmonary stenosis that disappeared within two years. She had slight motor delay but marked language delay, and she fulfilled criteria for ASD at age 4. Cerebral MRI showed asymmetric cranium and a slightly larger left hemisphere. At age 4.5 she was put in foster care, and was then weaned off diapers, learned to run and her language improved quickly. At age 8 years, her cognitive level was tested and it was determined that she has learning disabilities, borderline to but not fulfilling criteria for mild intellectual disability, and she is able to read. She also has problems with attention and social interaction. At 8 years of age, her height is +0.56 SD and OFC is +2.71 SD. She has small ears with attached ear lobule and retrognathia. Both sisters have everted lower lip, small alae nasi and fetal fingerpads on thumbs. They both learned to ride a bike at age 5.5.

The younger sister (8a), of whom less childhood information is available, had a reactive attachment disorder that was obvious from early age. Her early development is said to be better than her elder sister. She had delayed speech. She had a systolic heart murmur, and a small muscular ventricular septal defect without haemodynamic significance was found. Motor development was mentioned as delayed at age 4. She has a pleasing personality and less social problems, and does not have autistic features. She has attention deficit and her cognitive levels are clearly delayed with learning disability, mild intellectual disability is not excluded and new assessment is planned. Her height at age 6 is +1.46 SD, and her OFC +3.35 SD.

Proband 9 *284kb Del*

The male proband was the first child of unrelated healthy Caucasian parents without family history. Pregnancy was marked by gestational diabetes and ultrasound monitoring showed hydramnios and decreased fetal movements. He was born at 37 weeks of gestation by caesarean section due to breech presentation, biometric parameters were 50 cm (-0.06 SD) for length, 3500 g (-0.1 SD) for weight, and 37 cm (+0.68 SD) for OFC. He presented a psychomotor delay with severe hypotonia: walking at 3 years of age, first words at 2 years of age, and first sentences at 5 years of age. On clinical examination at the age of 7 years, parameters were: height 131 cm (+1.7 SD), weight 22 kg (-0.41 SD), and OFC 55 cm (+2.17 SD). He presented mild intellectual deficiency (mostly slowness), sleep disturbance, chronic constipation, diffuse articular hyperlaxity, scoliosis treated by orthopaedic corset, and velvet skin. He needed special education at 6 years of age. He had minor facial dysmorphic features such as long and flat face, up-slanting palpebral fissures, malar hypoplasia, opened mouth, and high arched palate. Fragile X syndrome screening, brain MRI at age 2 years and a half, and 4 years and a half and heart ultrasounds were normal.

Proband 10a and 10b *312kb Del*

Proband 10a was first seen as an 11 year old girl with mild intellectual disability, a large head (59.5 cm; +6.01 SD), high forehead, anteverted nares and a broad nasal tip. No cause was identified. She had a history of histiocytosis in her skull; at age 7 years she was treated for this condition with radiotherapy and made a full recovery. She coped within the regular school system with extra help but was significantly less academic than her parents and siblings. She was reviewed at age 20 years. Further investigations were again undertaken but no cause found. She had brief employments in retail but finds routine work difficult. She re-presented at 25 years of age when she was 21 weeks pregnant.

Proband 10b was the daughter of proband 10a. She was born by normal delivery with a birth weight 3.4 kg (-0.05 SD) and OFC 37 cm (+1.22 SD). There were no neonatal problems and her early milestones were normal. At 3 months the baby strongly resembled her mother facially with anteverted nares and a high forehead. Her weight and length were on 50th centiles but OFC on 90th centile. She made normal progress in the first few months, she sat at six months, bottom shuffled at 13 months and walked at 22 months. At 2 years 9 months she is speaking in sentences. Her height remains on the 50th centile, her weight is on 91th centile but her OFC (55.5 cm) is +4.60 SD above the mean. She required surgery for bilateral inguinal hernias, ligation of a PDA and blocked tear ducts.

Proband 11 *1.5 Mb Del*

The 8 years 4 months old boy is the only child of non-consanguineous Caucasian parents. He was referred for delayed language and pervasive development disorder. His mother had a personal and familial history of breakdown. He was born eutrophic after an uneventful pregnancy, at 39 weeks of gestation. He had feeding difficulties during the neonatal period. Motor milestones were not delayed, the boy was able to walk at 15 months. By contrast, language was severely delayed, however, by 8 years old the proband was no longer impaired. He also had attention deficit and anxiety disorder. Electroencephalography showed no sign of seizure. At examination, dysmorphic features included down-slanting palpebral fissures, deep-set eyes, blepharophimosis, broad nasal tip, thin upper lip and small ears without lobule. The boy also had brachydactyly, finger pads and transverse palmar crease. Height corresponds to +0.62 SD, weight to -0.04 SD and OFC to +0.15 SD.

Proband 12 *1.6Mb Del*

The proband is a 32-year-old male. His biological family history is unknown because he was adopted at birth. At three months of age he presented with macrocephaly (OFC +4.46 SD) leading to a CT scan showing agenesis of the corpus callosum. An MRI done at 21 months of age confirmed the diagnosis of complete agenesis of the corpus callosum. A follow up MRI performed when the proband was 21 years old also showed complete ACC with associated parallel orientation of the lateral ventricles, colpocephaly, Probst bundles, and prominence of the third ventricle. Seizures were suspected at one point, but an extended EEG was unrevealing, and he had no recurrence. This proband was delayed developmentally; at 21 months he was walking on his knees and did not begin to walk on his feet until 28-30 months of age. He also had difficulties with balance. He received physical therapy up to age 12, and currently attends occupational, speech and language, and psychological therapy once a week. He has never had any problems with his vision or hearing. He is somewhat insensitive to pain and has dysregulated core temperature with associated hyperhydrosis. He has elevated blood pressure (140/90) for which he takes medication. He has diagnoses of ADHD and learning disability. He has also impulse control problems and trouble gauging emotion in others. He took Ritalin up to age 14, then Adderall 40 mg 1x/day. Other medications include Prozac 40 mg 1x/day and Depakote ER 500 mg 1x/day. Upon a neurological exam at 21 years of age, his upper and lower limb reflexes were abnormal as well as his extraocular movements. At age 21, his head circumference was 61.5 cm. At age 22, he had a full-scale IQ of 88, a Verbal IQ of 95 and a Performance IQ of 79.

Proband 13 *2.4Mb Del*

This 7 year 10 months old girl was the first of two children of a non-consanguineous, healthy couple with unremarkable family history. The girl was born after an uneventful pregnancy at 41 weeks of gestation with a length of 56 cm (+2.38 SD), weight of 4030 g (+1.32 SD), and an OFC of 37 cm (+1.22 SD). She was reported to have recurrent infections including several pneumonias and frequent otitis media during early childhood. Initial developmental milestones were reported normal, but speech delay became apparent at the age of 24 months. At the age of 3 years global developmental delay, intellectual disability and behavioral abnormalities (temper tantrums, aggression) were diagnosed. The proband's speech improved with speech therapy; receptive language skills appeared to be less delayed than expressive speech. She attended a school for special needs, and was reported to be friendly, sociable and diligent. At the age of 6 years 5 months, a global IQ of 45 was determined by formal testing using HAWIK. An MRI of the brain at the age of 3 years 8 months revealed complete agenesis of corpus callosum and slightly enlarged cerebral ventricles.

On clinical examination at the age of 7 years and 10 months, her height was 137 cm (+2.68 SD), her weight was 43.9 kg (+3.82 SD), and her head circumference was 57 cm (+4.39 SD). Slight facial anomalies were noted including down-slanting palpebral fissures, sparse lateral eyebrows, high and narrow nasal bridge, flat philtrum, thin upper and thick lower lip, small ears, and slightly retrognathia (Figure 1A). Moreover the proband showed an inverted nipple on the left side, long fingers and toes, flat feet, and bilateral sandal gaps. She had muscular hypotonia but no specific neurological deficits.

Proband 14 *4.3Mb Del*

The proband was a 17 year old female and the only child of non-consanguineous Caucasian parents. She had four maternal and paternal healthy half-siblings. She was born at term after an uneventful pregnancy; her birth weight was 3200 g (-0.58 SD). She was a slow feeder and had recurrent infections in infancy. She reached all early motor developmental milestones appropriately. However, her speech development was delayed and she also had articulation difficulties. Bilateral mid-ear effusions were treated with grommets, and she also had a tonsillectomy. At the age of 5 years she developed bilateral esotropia, which was surgically corrected on three occasions. She was also prescribed glasses for hypermetropia. She had mild learning difficulties and an attention deficit, and needed some extra support in a mainstream school. She displayed episodes of challenging behavior. When assessed at the age of 8 years and 11 months, her height and weight were on the 25th centile and her OFC on the 75th centile. She had bilateral esotropia, significant epicanthic folds, short narrow palpebral fissures and sparse lateral eyebrows (Figure 1A). Her ears were small with flat upper helices and the right was low set. She had a small nose, narrow nasal bridge, a small mouth and an everted lower lip. Her hands showed mild radial deviation of the 4th distal phalanges, broad thumbs and fetal finger pads. Her 2nd toes were longer than her halluces, and she had very short 4th and 5th metatarsals. There was mild hypertrichosis on her lower back and lower legs. Her abdomen was distended, but there was no evidence of organomegaly. Muscular tone was reduced. At a subsequent assessment at the age of 16 years and 11 months she was post pubertal. Her height was on the 75th centile, and her weight and OFC were between the 50th and 75th centile. Additional features included mild shortening of the 4th and 5th metacarpals. She also had a systolic murmur on cardiac auscultation. An echocardiogram revealed a bicuspid aortic valve and mild tricuspid valve regurgitation. The distal limb anomalies were similarly present in her mother who was otherwise healthy and probably represent a familial form of Brachydactyly Type E.

Proband 15 *4.9 Mb Del*

The proband was the second child of healthy, non-consanguineous Caucasian parents. His birth weight was 3200 g at a gestational age of 40 weeks. He had feeding difficulties and had crying spells for several months. A developmental delay became apparent at the age of 9 months due to little social interaction and a mild delay in motor development. He had trigonocephaly with surgical correction at the age of 1 year. Speech development was severely delayed until the age of 5, despite intensive speech therapy. He suffered from recurrent ear infections and had unilateral cryptorchidism. At the age of 4 years old he was diagnosed with ASD by an expert multidisciplinary team. He had auditory sensitivity, was very anxious and had a psychotic episode at the age of 8 years old. He had a mild developmental delay, a friendly personality with an impairment of social interaction and very little eye contact. Clinical examination at the age of 10 shows facial dysmorphism with short and narrow palpebral fissures, sparse eyebrows and epicanthic folds. He has a long philtrum, a high narrow palate and small low set ears. He had a distended abdomen with weak abdominal muscles and normal body proportions.

Fetal case *p.(Ser356Leu)*

This case is a 29-gestational week male fetus of non-consanguineous parents. His mother has a manic-depressive illness. The pregnancy was obtained by insemination. At the first trimester, ultrasound revealed cervical hygroma. The karyotype performed on chorionic villi was normal (46, XY), as well as early echocardiography. Following ultrasounds showed an incomplete regression of the nuchal hygroma. At 22 weeks of gestation short corpus callosum, pulmonary sequestration and facial dysmorphism were noted. A CGH array was performed on amniotic fluid sample and revealed no genomic alteration. After genetic counselling, the couple asked for termination of pregnancy that was performed at 29 weeks according with the French Law. Fetal examination showed a male fetus with growth parameters at the high limits of standards for weight (95^{th} centile) and head circumference (90^{th} centile), and normal height (50^{th} centile). Facial dysmorphism included high and narrow forehead, down-slanting palpebral fissures, synophris, and hypertrichosis of face and upper chest. He had low set thumbs, broad halluces and hypoplastic nails. Autopsy showed pulmonary sequestration with two pulmonary lobes on both side, and revealed an auricular septal defect. Neuropathological examination showed a brain weight at 95^{th} centile and a short but thick corpus callosum with no other brain malformation.

Supplemental Figures

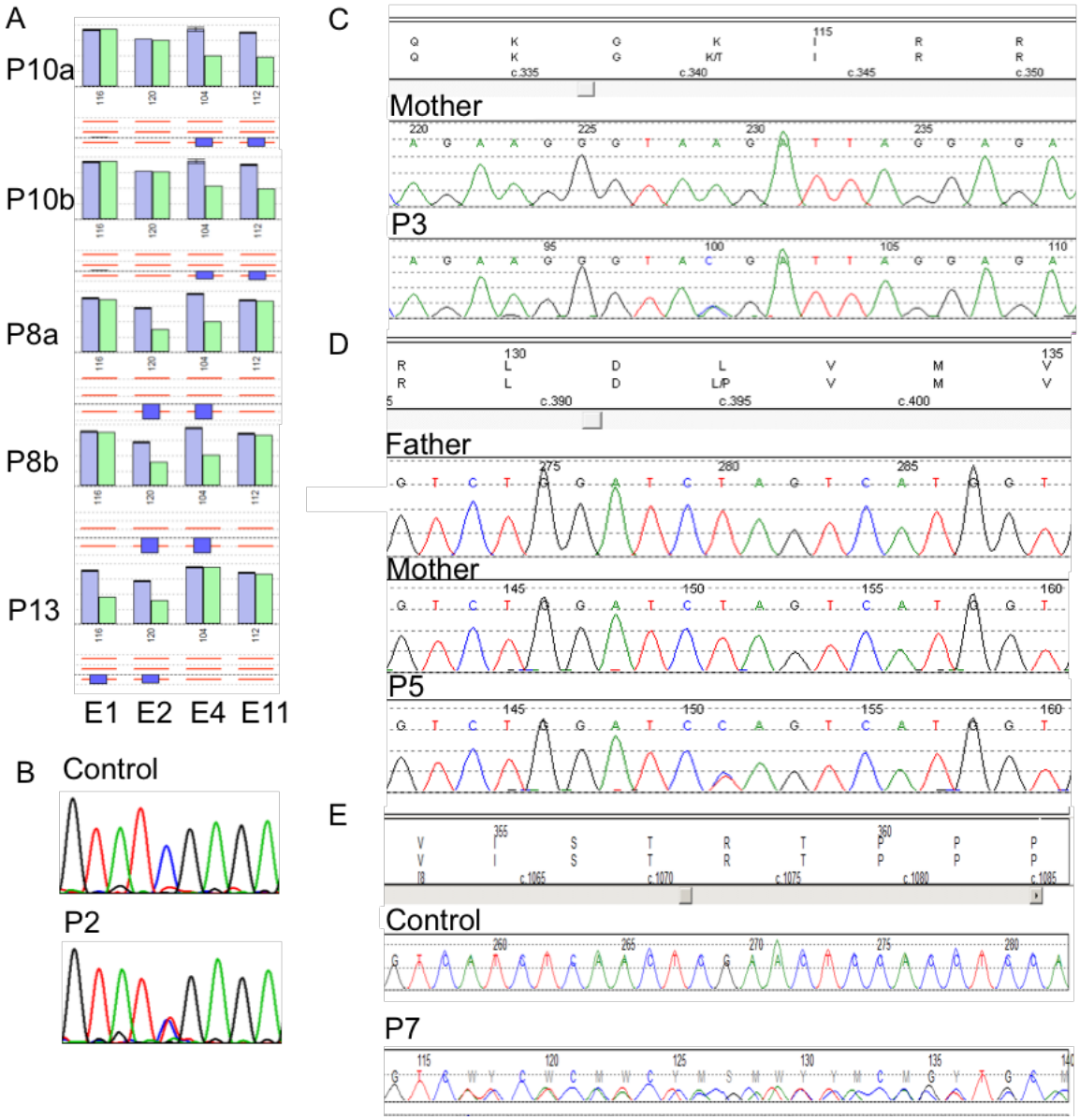

Figure S1 Additional information for *NFIB* deletion and sequence variation

(A) MLPA results for individuals 10a (mother) and 10b (daughter) showing a heterozygous deletion of exons 4 and 11 indicating the intragenic deletion breakpoint between exons 2 and 4. The intragenic deletion in individuals 8a and 8b was validated by MLPA analysis showing a heterozygous deletion of exons 2 and 4 but not of exons 1 and 11. MLPA result for individual 13 showing a heterozygous deletion of exons 1 and 2 also indicates the intragenic deletion breakpoint between exons 2 and 4. (B) Electropherogram demonstrating the heterozygous nucleotide exchange c.265C>T in exon 2 of the *NFIB* gene in individual P2, but not in a control individual. (C) Electropherogram demonstrating the heterozygous nucleotide exchange c.341A>C in exon 3 of the *NFIB* gene in P3, but not in his mother. (D) Electropherogram demonstrating the heterozygous nucleotide exchange c.376A>G in exon 5 of *NFIB* in individual P5 but not in his parents. (E) Electropherogram demonstrating the heterozygous nucleotide change c.1063_1076del in exon 8 in individual P7, but not in a control individual.

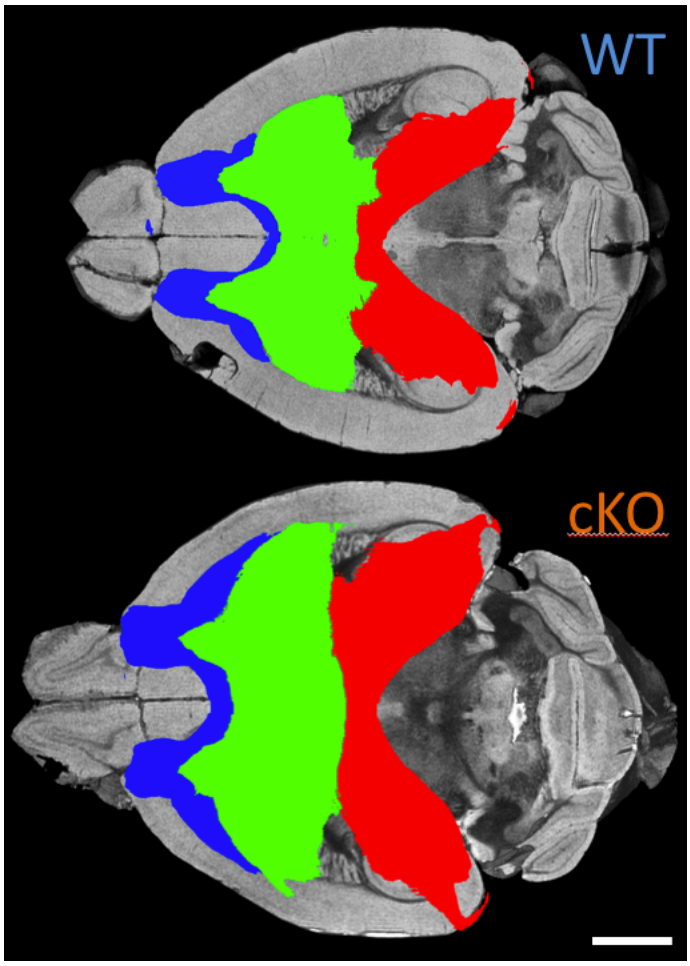

Figure S2 Additional information for tractography in mouse model.

Streamline density maps depicting the interhemispheric connectivity across the corpus callosum in an exemplar wildtype (WT; top) and dorsal telencephalon specific *Nfib* conditional knockout (cKO; bottom) mouse brain. The maps were derived from a probabilistic (iFOD2) diffusion fiber tractogram, seeded in the genu (green), body (blue) and splenium (red) of segments of the corpus callosum, respectively. Scale bar is 3 mm.

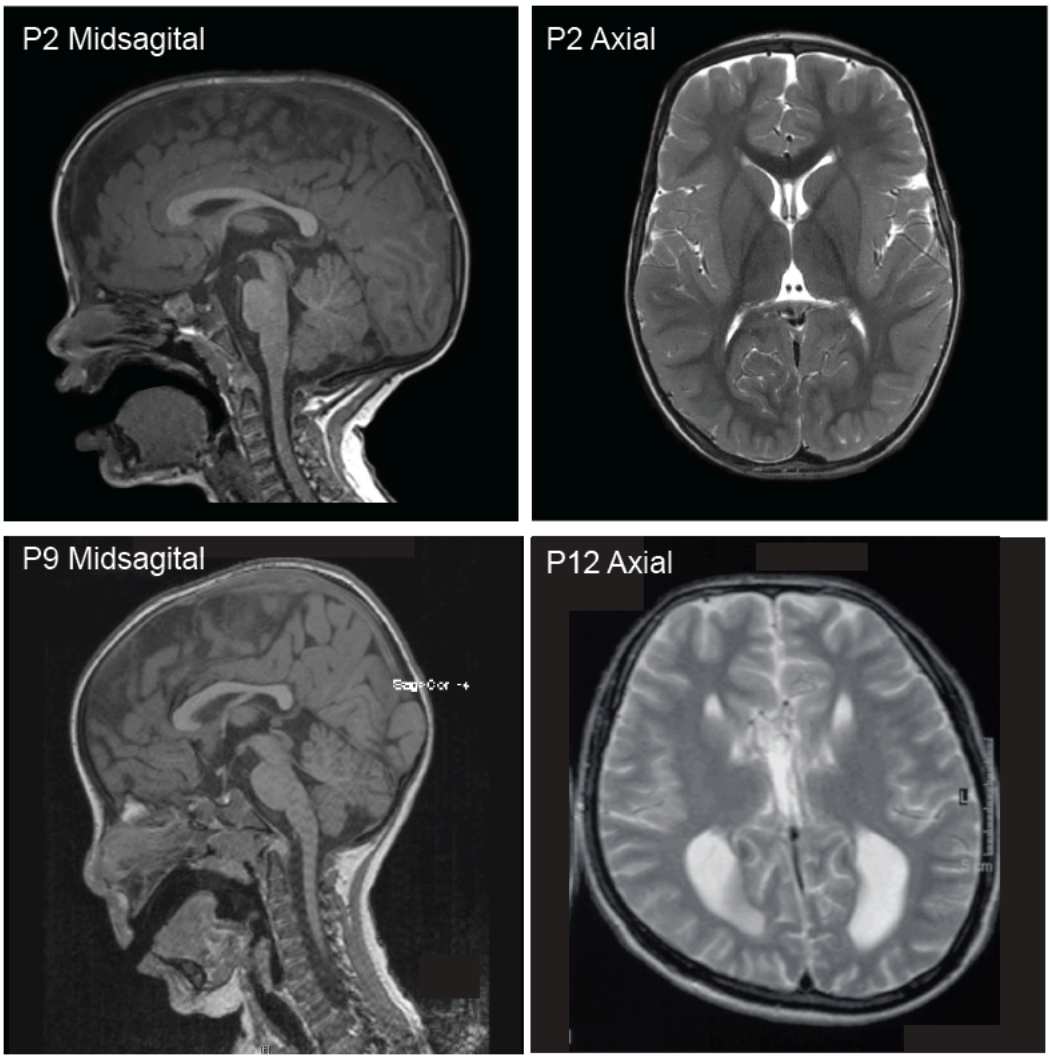

Figure S3 Additional brain imaging of individuals.

Midsagital and axial MRI images of P2, P9 and P12.

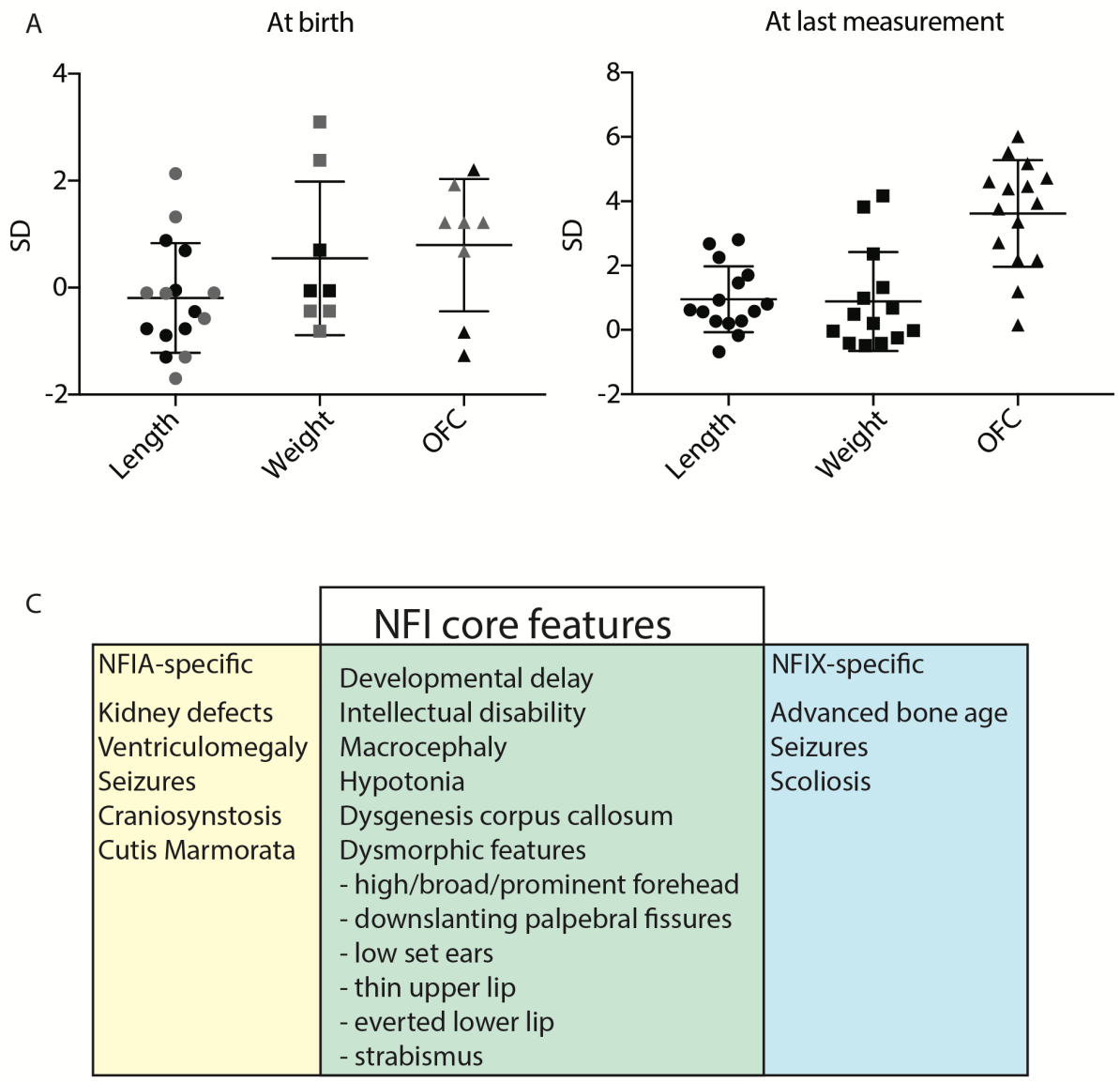

Figure S4 Clinical characteristics.

Dotplot representing the standard deviation (SD) of the growth parameters at birth (A) and at last measurement (B) based on information represented in Table 1. Grey dots represents individuals born prior to term or without this information available. (C) Schematic representation of the overlapping and distinct features of individuals with *NFIA*, *NFIB* or *NFIX* heterozygous sequence variants or deletions. Features in italic are reported in less than half the cases in literature.

Table S1: Primers used for cloning mutation

mutNFI_clon_F	TGCTGGTTATTGTGCTGTCTCA
mutNFI_clon_R	GGGGCGGAATTTACGTAGC
mutNFIB_K114T_F	GACCAGAAGGGTACGATTAGGAGGATCG
mutNFIB_K114T_R	CGATCCTCCTAATCGTACCCTTCTGGTC
mutNFIB_K126E_F	GACAGGCAGACGAAGTCTGGCGTCTGGATC
mutNFIB_K126E_R	GATCCAGACGCCAGACTTCGTCTGCCTGTC
mutNFIB_L132P_F	CAGGATCACCATGACTTGATCCAGACGCCAGAC
mutNFIB_L132P_R	GTCTGGCGTCTGGATCAAGTCATGGTGATCCTG
mutNFIB_S356L_F	CGCACAGTGTCATCTTAACTCGAACTCCAC
mutNFIB_S356L_R	GTGGAGTTCGAGTTAAGATGACACTGTGCG

Table S2: *In silico* predictions of consequence of NFIB sequence variants

Amino acid change	**p.(Arg37*)**	**p.(Arg89*)**	**p.(Lys114Thr)**	**p.(Lys126Glu)**	**p.(Leu132Pro)**	**p.(Asn254*)**	**p.(Ile355Serfs*48)**	**p.(Ser356Leu)**
HG19 chr9 position	14307441	14307285	14307210	14307174	14307155	14150191	14120603-14120622	14120617
Nucleotide change	G->A	G->A	T->G	T->C	A->G	C->CAC	del ATCTCAACTC GAACTCCACC	G->A
PredictSNP2	Deleterious	Deleterious	Deleterious	Deleterious	Deleterious	NA	NA	Deleterious
expected accuracy	0.77	0.93	0.87	0.87	0.87	NA	NA	0.87
CADD	Deleterious	Deleterious	Neutral	Neutral	Neutral	NA	NA	Deleterious
expected accuracy	0.6	0.56	0.56	0.61	0.56	NA	NA	0.8
DANN	Deleterious	Deleterious	Deleterious	Deleterious	Deleterious	NA	NA	Deleterious
expected accuracy	0.66	0.87	0.6	0.71	0.7	NA	NA	0.77
FATHMM	Deleterious	Deleterious	Deleterious	Deleterious	Deleterious	NA	NA	Deleterious
expected accuracy	0.64	0.95	0.62	0.6	0.65	NA	NA	0.83
FunSeq2	Deleterious	Deleterious	Deleterious	Deleterious	Deleterious	NA	NA	Deleterious
expected accuracy	0.65	0.93	0.61	0.61	0.61	NA	NA	0.61
PolyPhen-2 HumDiv	NA	NA	Probably damaging	Probably damaging	Probably damaging	NA	NA	Probably damaging
probability	NA	NA	0.991	0.979	0.997	NA	NA	0.985
PolyPhen-2 HumVar	NA	NA	Probably damaging	Probably damaging	Probably damaging	NA	NA	Probably damaging
probability	NA	NA	0.988	0.982	0.996	NA	NA	0.966
Mutationtaster	Disease causing	Disease causing	Disease causing	Disease causing	Disease causing	Disease causing	Disease causing	Disease causing
PROVEAN	NA	NA	Deleterious	Deleterious	Deleterious	NA	NA	Neutral
SIFT	NA	NA	Damaging	Damaging	Damaging	NA	NA	Damaging

Supplemental Methods

MR image acquisition

Magnetic resonance (MR) images were acquired for both WT (n = 3) and NFIB conditional knockout (n = 4) mouse brains at P110. The MR imaging was conducted using a 16.4 Tesla vertical bore, small animal MRI system (Bruker Biospin, Rheinstetten, Germany; ParaVision v5.0) which was equipped with Micro 2.5 imaging gradient and a 15 mm linear, surface acoustic wave coil (M2M, Brisbane, Australia). The protocol included both fast low-angle shot (FLASH) and diffusion-weighted spin-echo magnetic resonance imaging (dMRI). Prior to MR imaging, each brain was immersed in a proton-free oil, Fomblin Y-VLAC (Y06/6 grade, Solvay, USA); oxygen was actively removed from each sample via vacuum pumping.

Parameters for the FLASH pulse sequence: MTX 654 × 380 × 280, FOV 19.6 × 11.4 × 8.4 mm (0.03 mm isotropic voxels), TR/TE 50/12 ms, flip angle of 30°. No image averaging was used. Acquisition time was 0.7 hours per brain. Parameters for the dMRI pulse sequence: MTX 196 × 114 × 84, FOV 19.6 × 11.4 × 8.4 mm (0.10 mm isotropic voxels), TR/TE 200/23 ms, δ/Δ 2.5/12 ms. Two B0 (b-value = 0 s mm^{-2}) images and 30 diffusion-weighted (b-value = 5000 s mm^{-2}) volumes were acquired for each brain. The 30 diffusion-gradient directions used were evenly distributed over a hemisphere using the electrostatic repulsion method. No image averaging was used. Acquisition time was 15.5 hours per brain.

MR image processing was performed on a high-performance computing cluster with 1600 CPU cores and 8TB of RAM housed at the Queensland Brain Institute. Prior to processing, the diffusion-weighted MR images were de-noised and corrected for bias field inhomogeneity using tools provided by MRtrix (v 3.0; www.nitrc.org/projects/mrtrix). Scalar diffusion metric images were generated via weighted least-squares diffusion tensor estimation, while fibre orientation distribution functions (fODFs) was estimated with MRtrix via a constrained spherical deconvolution (CSD) model using the default pre-processing parameters (maximum spherical harmonic order lmax = 6). The response functions required to generate the fODFs were estimated using an iterative algorithm for single-fiber voxel selection.[81]

Brain measurements

Brain orientation was standardized between mice using an in-house script (MATLAB R2014a, Mathworks, California) to rotate the images to minimize the yaw and roll of each brain relative to the midline fissure. The pitch of each brain was then manually adjusted to ensure that an axial plane would intersect the center of the anterior commissure and the caudal tip of lobule IX of the cerebellar vermis. Measurements were made in either the midsagittal plane, or the coronal plane at Bregma level -2.18 mm.

These measurements included the cortex length and area in the midsagittal plane, and the cortex height in the coronal plane as represented in Figure 4D. The cortex length and area were normalized using the distance between the rostral tip of the cortex (the frontal pole) and the caudal tip of lobule IX of the cerebellar vermis in the midsagittal plane; the cortex height was normalized using the vertical distance between the dorsal edge of the cortex and the ventral edge of the hypothamalus.

Tractography

CSD-based probabilistic tractography, utilizing the iFOD2 algorithm, was performed on each brain.[55] The tractograms consisted of 200 thousand streamlines, and were created using the following parameters: maximum number of attempts = 1 million, fODF cut-off = 0.1, step size = 50 μm, maximum streamline length = 0.5/40 mm. The tractograms were seeded in either the midsagittal anterior commissure, or the midsagittal corpus callosum; the seed regions were contralaterally paired with inclusion regions (offset by several voxels on either side of the midline) to ensure streamlines connected the brain hemispheres. The seed regions were conservative in size in order to avoid seeding streamlines in the surrounding grey matter. Homotopic streamlines connecting the anterior cingulate cortices were also isolated in the corpus callosum tractograms, as was conducted in a previous study.[54]

Supplemental acknowledgements

Members of the International Research Consortium for the Corpus Callosum and Cerebral Connectivity (IRC^5, https://www.irc5.org) are listed as follows: Vicki Anderson (Murdoch Children's Research Institute, Melbourne, Australia); Tania Attié-Bitach (Hospital Necker-Enfants Malades and Université Paris Descartes, Paris, France); Warren Brown (Travis Research Fuller Institute, Fuller Graduate School of Psychology, Pasadena, CA); Christel Depienne (Université Paris Descartes, Paris, France); Delphine Heron (Université Paris Descartes, Paris, France); Roberto Lent (Federal University of Rio de Janeiro, Brazil); Richard J. Leventer (Murdoch Children's Research Institute, Melbourne, Australia); Paul J. Lockhart (Murdoch Children's Research Institute, Melbourne, Australia); Simone Mandelstam (Florey Neurosciences, Melbourne, Australia); George McGillivray (Murdoch Children's Research Institute, Melbourne, Australia); Lynn K. Paul (California Institute of Technology, Pasadena, CA); Linda J. Richards (The University of Queensland, Queensland Brain Institute and School of Biomedical Sciences, Brisbane, Australia); Gail Robinson (The University of Queensland, School of Psychology, Brisbane, Australia); Elliott H. Sherr (University of California, San Francisco, CA); Fernanda Tovar-Moll (Federal University of Rio de Janeiro and D'Or Institute for Research and Education).